DOE/SR/18035--T2

December 15, 1994

To The Graduate School:

This thesis entitled "XRF and Leaching Characterization of Waste Glasses Derived from Wastewater Treatment Sludges," and written by Robert G. Ragsdale, Jr., is presented to the Graduate School of Clemson University. I recommend that it be accepted in partial fulfillment of the requirements for the degree of Master of Science with a major in Environmental Systems Engineering.

Thomas J. Overcamp
Thesis Advisor

We have reviewed this thesis
and recommend its acceptance:

James Plesce

Robert A Fjeld

Accepted for the Graduate School:

Celine M. Lavin

AC09-89SR18035

XRF AND LEACHING CHARACTERIZATION OF WASTE GLASSES DERIVED FROM WASTEWATER TREATMENT SLUDGES

A Thesis

Presented to the

Graduate School of

Clemson University

In Partial Fulfillment

of the Requirements for the Degree of

Master of Science

Environmental Systems Engineering

---

by

Robert G. Ragsdale, Jr.

December 1994

ABSTRACT

The purpose of this study was to investigate using x-ray fluorescence (XRF) spectrometry as a near real-time method to determine melter glass compositions. As part of this effort, a range of glasses derived from wastewater treatment sludges associated with Department of Energy (DOE) sites was prepared. These glasses were analyzed by XRF and by wet chemistry digestion with Atomic Absorption/Inductively Coupled Emission Spectrometry (AA/ICPES). The results indicated good correlation between these two methods. Also, a rapid sample preparation and analysis technique was developed and demonstrated by acquiring a sample from a pilot-scale simulated waste glass melter and analyzing it by XRF within one hour. Based on these findings, XRF shows excellent potential as a process control tool for waste glass vitrification.

Glasses prepared for this study were further analyzed for durability by Toxicity Characteristic Leaching Procedure (TCLP) and Product Consistency Test (PCT) and the results are presented.

DEDICATION

To my Mother and Father and my wife, Sandi. To Mom and Dad for teaching me about values, personal responsibility, and setting goals. To my wife Sandi for encouraging me and having the patience to allow me to pursue this ambition.

ACKNOWLEDGMENTS

I would like to thank my committee members for their efforts in my behalf: Thomas J. Overcamp, Robert A. Fjeld, and James L. Resce. The work in this thesis was developed under the United States Department of Energy, Office of Technology Development, Mixed Waste Integrated Program Contract No. DE-AC09-89SR18035. I sincerely appreciate their support for this project. I would also like to acknowledge my appreciation for my funding from the South Carolina Universities Research and Education Foundation under Cooperative Agreement No. 8.

In addition, I would note the daily advice, assistance, patience, and encouragement provided by my research advisor, Jim Resce.

I would especially like to thank Westinghouse Savannah River Company (WSRC) for their support as well as Dennis F. Bickford for his guidance and assistance through the all important initial phase of concept design and implementation; Art J. Jurgensen for his extensive support of the XRF portion of the research; and Connie Cicero, not only for her assistance with the sample analyses, but also for serving as my contact and liaison at WSRC.

This project could not have been completed without the support from all these people.

TABLE OF CONTENTS

Table of Contents (Continued)

LIST OF TABLES

List of Tables (Continued)

List of Tables (Continued)

LIST OF FIGURES

CHAPTER I

INTRODUCTION

Vitrification is an emerging technology to incorporate inorganic hazardous and radioactive waste constituents into a glass matrix. Twelve metals with either a toxicity characteristic (40 Code of Federal Regulations (CFR) 261.24) or a listing under the Land Disposal Regulations (40 CFR 268.41 are designated as inorganic hazardous constituents. These metals are antimony, arsenic, barium, beryllium, cadmium, chromium, lead, mercury, nickel, selenium, silver, and thallium. Among the more common radioactive waste constituents are ^{137}Cs, ^{99}Tc, ^{235}U, ^{239}Pu, and ^{90}Sr.

To ensure that the durability of the glass meets regulatory specifications, the elemental composition of the melt must be closely monitored. This will ensure that variation in the melt composition, due to possible feed inhomogeneities, does not result in a deterioration in glass durability sufficient to require costly reprocessing. To prevent this occurrence, timely compositional analysis of the melt is a necessity.

By its very nature, process control requires dynamic and timely inputs in order to provide the feedback necessary to maintain the process within its design parameters. X-ray fluorescence spectrometry (XRF) is a very rapid analytical technique. Because of this, XRF lends itself well to application in process control.

The objectives of this project are to:

1. develop a molten glass sampling method, applicable to on-line melter operations, to make disks for XRF spectrometric elemental analysis;
2. demonstrate significant decrease in compositional analysis time through the use of XRF spectrometry versus digestion with AA/ICPES analysis;
3. compare conventional wet chemistry digestion with AA/ICPES analysis with XRF analysis of these waste glasses;

3. develop a procedure for making consistent constant surface area waste glass forms appropriate for Toxic Characteristic Leaching Procedure. (TCLP) testing;

4. test the leaching behavior of these glasses with TCLP and PCT. A detailed examination of the TCLP and PCT data is not part of this thesis.

The primary goal of this research is to evaluate the possibility of using x-ray fluorescence spectrometry as a more time efficient method to determine in near real-time the melter glass composition.

CHAPTER II

BACKGROUND AND LITERATURE REVIEW

Vitrification is leading edge technology that may solve previously 'difficult to solve' problems in hazardous waste disposal. Two very important advantages of vitrification are the significant volume reduction and a real potential for delisting of the associated hazardous material. The reduction in the complexity of disposal in terms of cost and sheer volume of space required is creating an enthusiastic response to vitrification technology. The Environmental Protection Agency (EPA) has declared vitrification to be the Best Demonstrated Available Technology for the disposal of high-level radioactive waste (Federal Register, 1990). Many waste streams are candidates for vitrification including baghouse dust, incinerator blowdown (Rescè *et al.*, 1994), incinerator slag, and high-level radioactive waste. Another important category of wastestreams is wastewater treatment sludges. Wastewater treatment sludges result from the treatment of previously used process waters to remove particulate matter and other undesirable constituents. The glasses produced and analyzed in this research project are intended to bear resemblance to glass products which might result from the vitrification of wastewater treatment sludges.

Wastewater Treatment Sludges

One source of this particular wastestream type comes from the hazardous and mixed sludges generated from wastewater treatment plants associated with Department of Energy (DOE) sites such as the Savannah River Site (SRS), Oak Ridge National Laboratory (ORNL), Rocky Flats Plant (RFP), and Los Alamos National Laboratories (LANL). Treatment of this aqueous wastestream is by the conventional process of precipitation, flocculation, and filtration to remove the dissolved metals. The filtered solids are placed in storage, awaiting further treatment and disposal. Generally, each of the DOE sites pursued a different precipitation method for the wastewater treatment.

These alternate precipitation methodologies, combined with differing original wastestreams, have produced sludges that vary in composition, sometimes dramatically, from site to site. The next section briefly describes and generally characterizes the surrogate of a sludge associated with an aqueous wastestream from each of these four major DOE sites. The purpose of these descriptions is to demonstrate the wide range of sludge compositional variability.

DOE's Savannah River Site (M-Area)

The primary source of this sludge from the Savannah River site (SRS) is a nickel plating line associated with nuclear weapons production. The total volume of the wastestream is approximately 1,200,000 gallons. After wastewater treatment, this volume is reduced by 65-70 volume % leaving 210,000 gallons of sludge and 450,000 gallons of newly created spent siliceous filter aid. The approximate oxide composition of a surrogate developed for this wastewater treatment sludge is shown in Table I. (Bennett *et al.*, 1994). The actual waste itself includes uranium and nitrate containing compounds.

Oak Ridge National Laboratory

An aqueous wastestream from the Oak Ridge National Laboratory (ORNL) site is the K-1407-B and K-1407-C ponds at the Oak Ridge K-25 site. These ponds were a holding/settling pond and a containment basin respectively. The approximate oxide composition of a surrogate developed for this wastewater treatment sludge are derived from these pond wastes and are shown in Table II (Bostick *et al.*, 1994). The actual waste includes uranium and organic matter.

Rocky Flats Plant

An example of a Rocky Flats Plant (RFP) low-level wastestream is the aqueous sludge from the plutonium recovery operations. The initial treatment used in the chemical precipitation of this wastestream used magnesium sulfate, ferric sulfate, calcium chloride,

Table I. SRS M-Area Surrogate Wastewater Treatment Sludge Composition

Oxide	Weight % (dry)
Al_2O_3	21.77
CaO	0.59
Fe_2O_3	1.10
MgO	0.25
MnO	0.35
Na_2O	13.51
NiO	1.16
SiO_2	54.33
Cr_2O_3	0.02
B_2O_3	0.04
TiO_2	0.06
K_2O	1.85
P_2O_5	4.03
BaO	0.03
PbO	0.13
ZnO	0.73
CuO	0.03
SUM	99.98

Table II. Oak Ridge National Laboratory Simulated Pond Waste Sludge Composition

Oxide	Oxide Weight % in Simulated Pond Waste (dry)
Na_2O	5.3
MgO	1.1
P_2O_5	1.3
Al_2O_3	15.9
BaO	0.1
CaO	69.8
Fe_2O_3	3.8
SiO_2	0.0
MgO	2.3
PbO	0.6
NiO	0.3
SUM	100.5

and coagulants. The filter press used in dewatering the sludge was coated with diatomaceous earth, a siliceous material. The approximate oxide composition of a surrogate developed for this wastewater treatment is shown in Table III (Cicero *et al.*, 1993). The actual sludge contains isotopes of U, Pu, and Am, as well as small amounts of Cr, Ni, Pb, Cd, Ag, and organic matter.

Table III. Rocky Flats Plant Sludge Surrogate Oxide Composition

Oxide	Weight % (dry)
Al_2O_3	1.61
B_2O_3	0.12
CaO	15.31
Fe_2O_3	56.19
K_2O	0.45
MgO	10.60
MnO_2	0.09
Na_2O	3.68
NiO	0.03
P_2O_5	0.04
PbO	0.02
SiO_2	6.73
TiO_2	0.01
ZnO	0.12
SUM	100.00

Los Alamos National Laboratory

Water is used at Los Alamos National Laboratory (LANL) as part of decontamination techniques. Treatment of this process water results in a mixed waste sludge. While the influent water contained about 100 mg/L of total dissolved solids (TDS), the wastewater contained about 1,000 mg/L of TDS. This wastestream was treated with around 2,000 mg/L of ferric sulfate and was precipitated with about 8,000 mg/L of calcium hydroxide (Bostick *et al.*, 1994). At one time, the dewatering equipment

used diatomaceous earth (DE) as a filter aid; but more recently, the process was adjusted to use perlite. While DE is primarily silica, perlite contains significant amounts of Al and K. The approximate oxide composition of a surrogate developed for this wastewater treatment sludge is shown in Table IV (Cicero, 1994). The actual sludge contains isotopes of U, Pu, and Am.

Table IV. Los Alamos National Laboratory Simulated Wastewater Treatment Sludge Composition

Oxide	Weight % (dry)
Al_2O_3	3.47
BaO	0.08
CaO	44.85
CdO	0.08
Ce_2O_3	0.13
Cr_2O_3	0.19
Fe_2O_3	6.67
MgO	4.35
NiO	0.09
PbO	0.07
SiO_2	40.02
SUM	100.00

The current inventory of this waste type is about 154 m^3, with an annual filter cake generation rate of about 52 m^3.

In order to make comparison of the compositions of the various wastestreams easier, Table V has been produced as a summary table highlighting the major constituents from the previous tables.

The waste, the precipitation method, and the filter aid all have a significant impact on the resultant sludge composition.

Table V. Summary of Major Oxide Constituents in the Wastestream Surrogates (in wt %)

Site	Precipitation Method	Na_2O	Al_2O_3	Fe_2O_3	CaO	SiO_2	MgO
ORNL	$Ca(OH)_2$	5	16	4	70	-	2
RFP	$Fe(SO_4)$, $CaCl_2$, $MgSO_4$	9	2	56	15	7	11
LANL	$Fe(SO_4)$, $Ca(OH)_2$	-	3	7	45	40	4
M-Area	NaOH	14	22	1	1	54	-

X-Ray Fluorescence Spectrometry

Introduction

XRF spectrometry is capable of providing both qualitative and quantitative inorganic chemical analysis of elements ranging from boron to uranium. A description of this technique is provided in this section. For a more in depth coverage of this subject, several good books have been written by Berstein (1962), Bertin (1970), Birks (1969), and Carr-Brion (1989).

The following factors tilt the balance significantly in favor of XRF spectrometric analysis. First, this is a nondestructive testing procedure. Also, XRF accepts a specimens in a variety of physical forms. For a solid sample, a highly polished flat surface is the ideal and yields the best results. However, XRF analysis can also be performed on liquids, powders, and objects of varied shapes such as washers, bolts, and other parts. It is extremely easy to use. It performs well with high precision and accuracy and is not time intensive. An accurate analysis of a solid matrix with a relatively large number of elements present may be obtained in minutes. Other analysis methods such as inductively coupled plasma emission spectrometry (ICPES) or atomic absorption (AA) analysis can take hours to complete since the sample must be digested into an aqueous matrix prior to presentation to the instrument. Because of the slow, tedious nature of AA and ICPES, they are not readily amenable to process control. On the other hand XRF is a leading

candidate for use as a process control tool. It was the purpose of this research to determine if XRF can provide the analytical speed, and accuracy, and precision necessary for use in process control.

Application of XRF to the commercial glass industry is quite extensive. However, there has been minimal use, to this point, of XRF in the area of waste glasses. Carney (1994) has used XRF to determine the composition of a vitreous surrogate slag in an attempt to quantify Ce, as an actinide surrogate, and Fe. He also used XRF to analyze the powdered processed standards which were made of Si, Al, Fe, and Mg. His conclusions were that "XRF technique shows promise for providing rapid semi-quantitative data for the Ce and the Fe in the slag material" (Carney, 1994). The oxides in his research, common to this thesis, were Fe in amounts from 0.0 to 16.7 weight percent, Al from 2 to 11 weight percent, and Si from 22 to 32 weight percent. By comparison, the oxide composition ranges used in this thesis are Fe from 4 to 35 weight percent, Al from 3 to 15 weight percent, and Si from 14 to 57 weight percent.

Physics of X-Rays

X-rays were discovered by W. C. Roentgen in 1895 and are produced by the bombardment of matter with protons, electrons, or heavier ions. Inner shell electrons of matter are preferentially removed by these particles. In moving to refill these inner shell vacancies, outer shell electrons give up energy in discrete quantities in a form called x-rays. This process of producing x-rays by the direct bombardment of matter with particles is called primary excitation. However, these resulting x-rays are further capable of striking a second atomic target and also cause an inner shell electron from that target to be ejected. This process produces an x-ray and is called secondary excitation or fluorescence.

The total number of the secondary excitations, for each individual element in the matrix, is termed the fluorescent intensity of that element and is usually expressed in

thousands of counts per second as recorded in the detector. The fluorescent intensity is proportional to several factors including. primary and secondary mass absorption coefficients, sample density, sample thickness, and the weight fraction of the element in the matrix. Equation (1) (Carr-Brion, 1989) shows the relationships of these factors to fluorescent intensity (I_F).

$$I_F = \frac{K I_O (1 - \exp[-(\mu_P - \mu_S)\rho x])}{\mu_P + \mu_S} W_a \qquad (1)$$

where K is a factor dependent on geometric yield, fluorescent yield, etc.,

I_o = the original intensity,

μ_P = the sum of the primary mass absorption coefficients.

μ_S = the sum of the secondary (fluorescent) mass absorption coefficients.

ρ = the density,

x = the sample thickness,

W_a = the weight fraction of element *a* in the sample.

The fluorescent intensity, with the proper detector, multi-channel analyzer, and counting circuitry, generates a line spectrum. The secondary excitation of a sample produces a line spectrum unique and proportional to each element present in the sample.

The penetration of x-rays into the sample is limited depending on the composition of the sample, the absorption coefficient associated with each element in the matrix, and the energy of the x-rays. It must also be considered that the x-rays created within the sample, that is the fluorescence, must escape in order to be detected. The lower the atomic number of the element in the matrix, the lower the energy of the fluorescent x-ray and the greater likelihood that the fluorescence will be absorbed prior to departure from the interior of the sample. Furthermore, these soft x-rays are much more likely to be absorbed enroute to or in the window of the detector. Therefore elements with low atomic numbers pose special problems. As the atomic number decreases, the region of analysis can decrease from a depth of several millimeters (mm) to several hundred angstroms. For

example. Na, B and other elements of lower atomic number produce very soft x-rays which have a very limited ability to escape the matrix and are also readily attenuated in air and in the detector window. Special considerations are necessary for these elements. Some currently implemented techniques include maintaining a vacuum or specialized gas like helium in the XRF sample chamber, use of ultra thin detector windows, use of more sensitive, more efficient liquid nitrogen cooled detectors, and use of higher power x-ray tubes which produce increased flux. Even with these precautions, low count rates may lead to excessively long counting times.

Instrumentation

A simplified diagram of the components of the interior of a wavelength dispersive XRF spectrometer adapted from de Galan (1990) is presented in Figure 1.

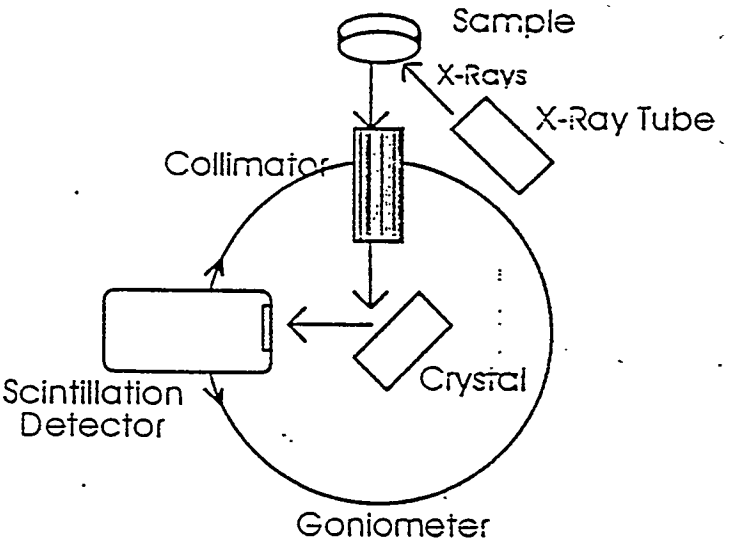

Figure 1. Typical Wavelength Dispersive X-Ray Fluorescence Spectrometer

Direct excitation occurs in the x-ray tube where electrons bombard a fixed target generating primary x-rays with an energy proportional to the mass of the target atom. The target is important in that the x-rays produced need to have sufficient energy to be able to

remove inner shell electrons and produce fluorescence in all the elements present in the sample. Chromium and rhodium are commonly used targets because they produces x-rays that will excite most materials. They are durable in the environment of the x-ray tube and are easily obtainable at high purity levels. These primary x-rays strike the sample and generate the secondary x-rays called secondary fluorescence. This is the characteristic radiation (or fluorescent intensity) that is unique to each of the elements present. The sum of the characteristic radiations is in the form of a polychromatic radiation which is then collimated into a nearly parallel bundle. The divergence from the collimator is usually the limiting factor in the resolution of the spectrometer. The collimated x-rays strike the analyzing crystal, which acts like a three-dimensional grating to diffract the x-rays. Since different secondary x-ray wavelengths require different crystal planar separations in order to be diffracted, several different crystal types are used specific to the element being analyzed. The more common crystals may be made from lithium fluoride, germanium, and other materials. Although Figure 1 depicts a single crystal, modern spectrometers have a number of different crystals that can be selected for optimizing the analysis for the element of interest. The crystal and the detectors are mounted on a goniometer. As the goniometer turns, the effective planar separation of the crystal shifts relative to the incident beam. Therefore, for each position of the crystal, a different single wavelength will be diffracted via constructive interference in accordance with Bragg's law.

$$n\lambda = 2d\sin\theta \qquad (2)$$

where n is the order of diffraction (usually n = 1),

λ = the wavelength,

d = the interplanar spacing of the crystal,

θ = the angle between the crystal and the incident radiation.

The incident radiation arrives at an angle of θ relative to the crystal surface. The diffracted radiation leaves the crystal at an angle of 2θ relative to the incident beam. This radiation is measured in the detector which is always positioned at an angle of 2θ relative

to the incident radiation as the crystal and detector is rotated from zero to ninety degrees in order to measure the entire spectrum from the sample (Birks, 1969).

Errors

The sources of error associated with the measurement of x-ray intensity fall into approximately six main categories as follows (Berstein, 1962):

1. Counting error - the error (or standard deviation) in the counts is the square root of the number of counts.

2. Instrument errors - include short and long term instabilities and drift in x-ray tube voltage and current; primary x-ray spectral distribution; temperature induced changes in the crystal interplanar spacing; changes in the detectors due to voltage fluctuations, and electronic noise.

3. Operational errors - primarily due to operator technique.

4. Specimen error - primarily non-homogeneity of the sample and absorption and enhancement effects. Absorption refers to the process by which the secondary x-ray is reabsorbed by the matrix before it can escape from the sample and be detected. This reduces the apparent fluorescent intensity for that particular element. The opposite process, enhancement, occurs when the fluorescence of one element has sufficient energy to excite one or more other elements in the sample (Birks, 1969). This creates an increase in the apparent fluorescence from a particular element in excess of that which would be attributed solely to the secondary excitation caused by photon bombardment from the x-ray tube.

5. Estimation error - occurs when determining the element concentration from the calibration curve.

6. Spectral-line interference - contributions from closely adjacent spectral lines to the spectral line of the analyte of interest.

Sample Preparation

Solids for XRF are prepared as pressed powders or fused glass disks. Powders can be mechanically pressed into a disk with the aid of a binder. This method can have particle size effects. These effects can be minimized by grinding the powder sufficiently fine. In most cases a -300 mesh powder is sufficient to produce good results. This can be verified by measuring the elemental intensities at several stages in the grinding process and

stopping when the intensity values reach a constant level (Birks, 1969). In the second form, particle size effects can be eliminated by fusing the sample with an appropriate flux (Claisse, 1957) and then casting into a non-wetting platinum/gold alloy mold or a graphite mold. Some materials do not require additional flux in order to be made into a castable melt.

The next step in the preparation of a solid fused sample is the annealing process. The molten sample is poured into a mold which yields a disk shaped form. As the sample disk cools, a temperature gradient is internally established. This creates longitudinal tension in the outer layers and leaves an area of no stress in the center of the sample. In order to relieve these stresses and prevent the disk from either spontaneously shattering or shattering with handling or polishing, it is necessary to anneal the disk. Alvarez (1990) describes a method to optically detect and measure the stresses in the fused XRF disk by use of a polariscope. Also, a method is described to determine the annealing time.

Graphite molds have been used in the fusion of geological samples (Luedemann *et al.*, 1991). The graphite mold does not create quite as smooth a surface as the platinum/gold alloy mold. However, it is easy to use, inexpensive, and does not require acid cleanup as is the case with metallic molds. While precision from a graphite mold cast sample is good, the best results are achieved by carefully polishing the disk. Usually a 600 grit dry polished surface is sufficient and produces excellent results. This surface, although very smooth, does have very fine parallel lines, whereas a sample poured into a platinum alloy mold does not. In order to avoid diffraction effects from these lines, the sample is spun inside the XRF.

To reiterate, two factors are very important in sample preparation. First, the sample must be homogeneous. Secondly, precise and accurate analyses require a flat and smooth sample surface.

Quantitative Analysis

The unique characteristic radiation produced from the sample can lead to quantitative evaluation of the elemental composition. However, the intensity or count rate, when plotted directly on a calibration curve of intensity versus elemental concentration, may be non-linear. The usual source of the non-linearity is due to inter-element effects, such as matrix effects like absorption and enhancement. The goal is to use a model that will correct this curve back to linearity. Relating fluorescent intensity to composition can be accomplished, to a greater or lesser extent, by one of two methods.

The first method of XRF quantification is called the empirical coefficients method and uses empirically determined coefficients relating one element's matrix effects on another. This requires the development of calibration curves from matrix-matched standards. The result is that the effect of each element on every other element in the matrix is measured. With this procedure, as the number of elements increase, the number of standards increases. Clearly, in a complex matrix, determination of the empirical coefficients can be a significant undertaking. The best results are obtained when the empirical coefficients are measured in a matrix similar to the that of the sample. Several variations of this type of empirical model improved through the years, were developed by a number of researchers. The Lucas-Tooth-Pyne model is optimized towards analysis of samples with small elemental concentration ranges (Lucas-Tooth and Pyne, 1964). The Rasberry-Heinrich model is claimed to give better fits when there are strong enhancement effects (Rasberry and Heinrich, 1974). It is suggested that the de Jongh model is able to give a better fit where both absorption and enhancement effects are present (de Jongh, 1973, 1979). Another widely used model is the Lachance-Traill models (Lachance and Traill, 1966). A modification of the Lachance-Traill model, able to handle one or two component systems as well as complex systems over a wide concentration range, has been constructed by LaChance and Claisse (1980). Each of these models requires extensive preparatory lab work and are computationally intensive.

The second method, called the fundamental parameters method, uses basic parameters such as x-ray tube power, include x-ray tube target material, tube voltage, tube window thickness, x-ray tube spectra, published x-ray mass attenuation coefficients, geometrical factors, and fluorescent yields, etc., to calculate the quantitative presence of the elements in a sample from the intensities. Fundamental parameters method, which significantly reduce the required number of standards, was brought to world attention through the work of Criss and Birks (1968). The only assumptions made for this model are that the sample is infinitely thick, has a flat surface, and is homogeneous. The composition is directly calculated by iteration (Birks, 1969). The results from the model are becoming increasingly more accurate as researchers more carefully measure the fundamental parameters. The advantage of this particular model is that composition can be calculated without the use of standards or empirical coefficients to a high degree of accuracy. Use of standards allows even better results. In order to allow more wide spread usage, the computer code for this model was rewritten so that it could be run on a personal computer (Criss, 1980).

Inductively Coupled Plasma Emission Spectrometry (ICPES)

The focus for this project is the use of XRF as a process control instrument in the field of vitrification. This section will provide a foundation to show that XRF would be a more productive analysis method.

Like the flame atomic absorption spectrometer (FAAS) and the graphite furnace atomic absorption spectrometer (GFAAS), the inductively coupled plasma emission spectrometer (ICPES) requires the sample to be in a liquid matrix.

Because the solid glass sample must be digested first, the total time required for analysis by ICPES is dramatically increased to several hours (analysis by wet chemical methods followed by ICPES and/or AA is hereinafter referred to as ICP). It is precisely

this that makes XRF analysis of waste glass so attractive. The average analysis time for XRF analysis is on the order of minutes. XRF application to process control is obvious.

CHAPTER III

STATEMENT OF EXPERIMENTAL OBJECTIVES

Table V shows a wide range of variability in the elemental composition of the example wastestreams. A prerequisite of this project is to derive a compositional space to encompass as many of the elemental extremes from the wastestreams of these wastewater treatment sludges as possible. Vitrification of compositions within this space will result in a series of glasses which will be evaluated as discussed later. The objectives of this research are to:

1. develop a molten glass sampling method applicable to on-line melter operations to make disks for XRF spectrometric elemental analysis,
2. demonstrate significant decrease in compositional analysis time through the use of XRF spectrometry versus digestion with AA/ICPES analysis,
3. compare conventional wet chemistry digestion with AA/ICPES analysis with XRF analysis of these waste glasses,
4. develop a procedure for making consistent constant surface area waste glass forms appropriate for Toxic Characteristic Leaching Procedure (TCLP) testing, and
5. test the leaching behavior of these glasses with TCLP and PCT. A detailed examination of these TCLP and PCT data is not part of this thesis.

The primary goal of this research is to evaluate the possibility of using x-ray fluorescence spectrometry as a process control tool to determine near real-time melter glass composition.

CHAPTER IV

EXPERIMENTAL PROCEDURE

Construction of the Compositional Space

The experimental design procedure used to construct the glass composition space examined in this research is described in this section. The major elements present in the wastes from the four DOE sites discussed in Chapter II include Si, Al, Fe, Ca, and Na. To these five elements B is added for glass forming properties and Ni, Pb, and Ba are added to represent the hazardous species.

After estimating the probable glass-forming region on the CaO-SiO_2-Fe_2O_3 ternary phase diagram (American Ceramics Society, 1969), several screening studies were performed to determine the actual limits suitable for vitrification. The screening studies demonstrated the need to decrease the Fe level in order to eliminate insolubilities within the melt. A large glass-forming region was predicted and is depicted as the rectangular area in the CaO-SiO_2-Fe_2O_3 ternary phase diagram shown in Figure 2. This region is defined by four vertices each with differing amounts of SiO_2, CaO, and Fe_2O_3. The orientation of the region on the phase diagram is such that only two levels of Fe_2O_3 are present. This leads to one level of Fe_2O_3 for points 1 and 2 and a higher level for points 3 and 4. The compositions of the vertices of this compositional space are shown in Table VI.

The significance of the Point 1 composition is its low Fe_2O_3, high CaO, and low SiO_2 content. Point 2 on the other hand has acomposition which is low in Fe_2O_3, and has the highest SiO_2 content. Point 3 has high Fe_2O_3 and CaO composition and it has the lowest level of SiO_2. Point 4 completes the compositional space as a composition with high Fe_2O_3 and SiO_2 contents and low CaO.

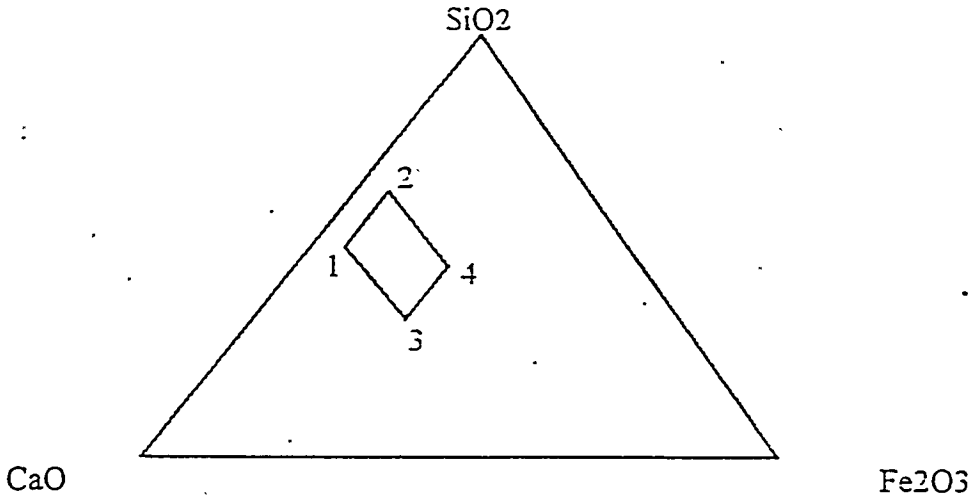

Figure 2. The CaO - SiO_2 - Fe_2O_3 Ternary Phase Diagram

Table VI. Summary of Major Constituents in the Original Composition in Mole Percent

Point	SiO_2 (Mole %)	CaO (Mole %)	Fe_2O_3 (Mole %)
1	42	54	4
2	63	33	4
3	35	45	20
4	56	24	20

This compositional space was expanded dimensionally by substitution of Na_2O for part of the CaO at two levels such that the two mole ratios of Na to Ca were 0.5 and 2.0. This doubled the original four vertices to a total of eight. In order to add B_2O_3 to the compositional space, an additional eight points were created. The B composition in these eight points was determined by substituting 17 mole percent B_2O_3 for SiO_2. This brought the number of vertices to sixteen. In order to add Al_2O_3 to the space, these 16 points were duplicated, but with a 10 mole percent substitution of Al_2O_3 for SiO_2. Thus, the final compositional space is defined by 32 points or vertices representing a five-dimensional hyperspace. Additionally, for all 32 compositions, Ba, Ni, and Pb oxides was added at the following fixed levels:

2.0 mole % Ni substituted for Fe;

2.0 mole % Ba substituted for Ca;

1.0 mole % Pb substituted for Ca.

After expansion of the compositional space, a series of glasses were prepared which corresponded to the vertices and some interior points of the space.

The naming convention for each of the points of the space follows. Each glass is identified by a number followed by three letters. The numbers can range from one to four and relates back to the original four vertices in Figure 2. The first letter relates to the level of Na in that glass with *L* suggesting a Na/Ca ratio of 0.5 and *H* suggesting a Na/Ca ratio of 2.0. The second letter relates to the level of B in that glass with *O* suggesting no B and *H* suggesting the high level. The third letter relates to the level of Al in that glass with *O* suggesting no Al and *H* suggesting the high level. The following example will clarify this concept. The glass 2LHO suggests that this is a derivative of Point 2. The first letter indicates that the Na/Ca ratio in the glass is 0.5, the second letter indicates that B_2O_3 has been substituted for 17 percent of the SiO_2, the third letter indicates that Al has been added.

The 2-Space defines a subspace of the entire composition space defined by 2LOO, 2HOO, 2LHO, 2HHO, 2LOH, 2HOH, 2LHH, and 2HHH.

The 2-Space is pictorially presented as a cube in Figure 3. This figure demonstrates the result of the substitutions applied to the original Point 2. For example, 2HHH would be derived from Point 2 with substitutions at high levels of Na, B, and Al. Increases in the substitution ratio of the various elements from the low value to the high value are indicated by arrows.

Points 1, 3, and 4 have similar three-dimensional depictions and exist within the compositional space. The general relationships between the subspaces are depicted in Figure 4. This figure represents a 5-dimensional space. One of the major differences between these subspaces is the increase in the Fe concentration indicated by the arrow.

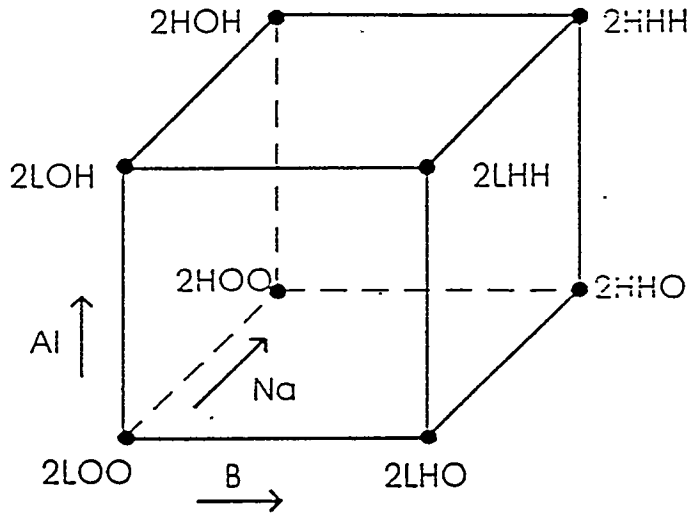

Figure 3. A Depiction of 2-Space

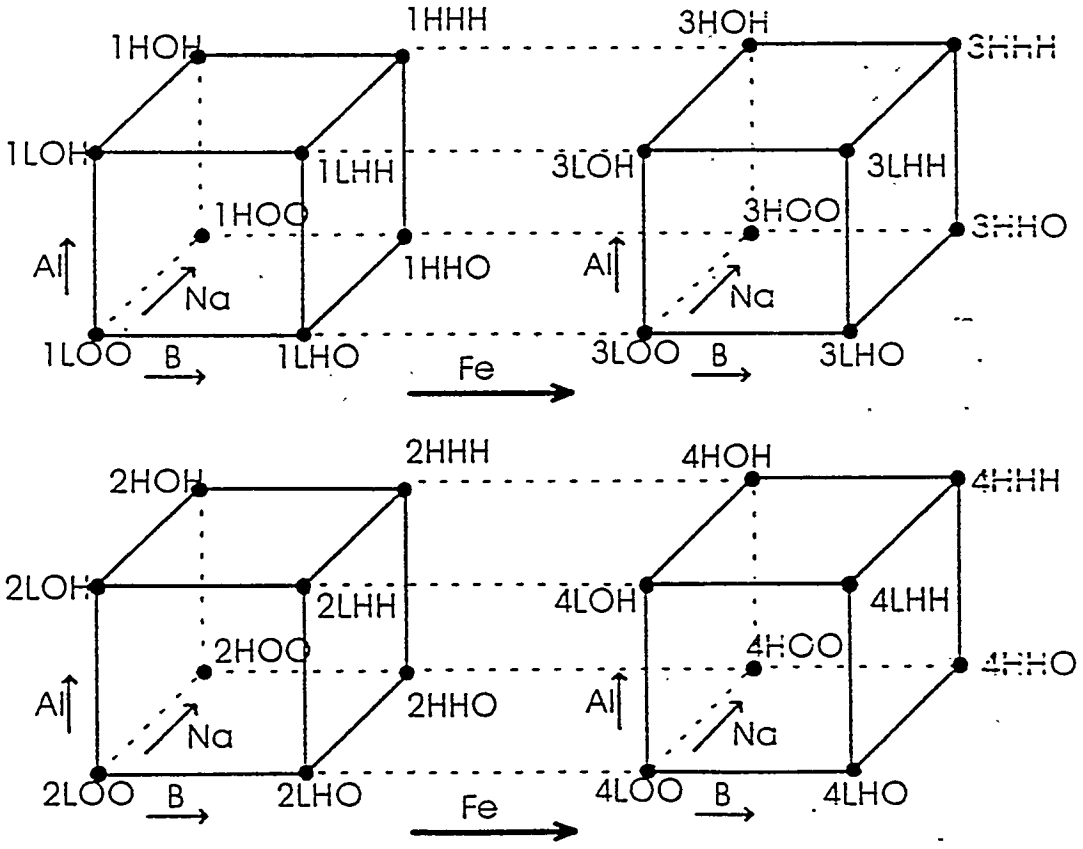

Figure 4. Relationship between the Subspaces

In addition to the 32 vertices, a decision was made to make three replicate glasses representing the midpoint of the entire compositional space. These glasses are called MID1, MID2, and MID3. Midpoints from several of the possible subspaces were also produced. For example, from Figure 3, the midpoint of the 2-Space is called 2MMM. It was constructed by taking equal masses of powdered glass from each of the eight points associated with the 2-Space. Because of some insolubilities in the 4-space glasses with alumina, these four compositions were mixed with their counterparts in 2-space and renamed as 6-space glasses. For example, 6LOH is a mixture of 40% 2LOH and 60% 4LOH. The remaining mixtures are 6HOH at 50% 2HOH and 50% 4HOH, 6LHH at 30% 2LHH and 70% 4LHH, and 6HHH at 25% 2HHH and 75% 4HHH. The weight percent compositions and the mole percent compositions associated with the compositional space are listed in the appendix in Tables A-I and A-II.

Chemicals

The chemicals required to make the points of the compositional space were silicon (IV) oxide, SiO_2, with a purity of >99.5% purchased from Johnson Matthey, Ward Hill, Maine; calcium oxide powder, CaO, reagent grade (purity of >99%) purchased from Mallinkrodt; sodium carbonate, Na_2CO_3, ACS grade (purity of >99%), purchased from Johnson Matthey, Ward Hill, Maine; iron (III) oxide, Fe_2O_3 , -325 mesh powder with a purity of >99.8% (metals basis) purchased from Johnson Matthey, Ward Hill, Maine; boron oxide, B_2O_3 , 60 mesh powder with a purity of >99%, purchased from Johnson Matthey, Ward Hill, Maine; barium carbonate, $BaCO_3$, 1 micrometer powder with a purity of >99.9% (metals basis) purchased from Johnson Matthey, Ward Hill, Maine: nickel (II) oxide, NiO, with a purity of >99%, purchased from Johnson Matthey, Ward Hill, Maine; and lead (II) oxide, PbO, powder with a purity of >99.9%, purchased from Johnson Matthey, Ward Hill, Maine.

Glass Preparation

A total of 43 glasses were prepared. These included the original 32 compositions which correspond to the vertices of the space plus an additional 11 glasses within the space. A concern throughout the project was to ensure homogeneity of the glass and to avoid contamination of the melts.

A volume of approximately 500 cm^3 of each glass was made. This quantity was adequate to not only make the required samples for each point, but also to leave a glass reserve to support possible future projects. Previous crucible tests suggested that glass density would be approximately 2.5 to 3.0 g/cm^3. This density suggested that around 1500 g of oxides would be required for each point. Using the weight percentages from the appendices, the required amounts of each oxide were calculated. In the melt, sodium carbonate decomposes to Na_2O with a release of CO_2. It was necessary to calculate the correct quantity of sodium carbonate required to compensate for this decomposition. The oxides for each glass were weighed on a Mettler™ PM6100 electronic scale to an accuracy of +/- 0.03 g. Prior to melting, the weighed oxides for each glass were placed in a Nalgene™ half gallon container which was rotated on a Model DC-20 TCLP Extractor made by the Analytical Testing Corporation of Warrington, PA, for at least three hours to ensure homogeneity of the mixture.

The powder was placed in 750 mL high purity alumina crucibles made by Coors Ceramics of Golden, Colorado. Because of concerns about the thermal sensitivity of the alumina crucible, this crucible was nested in a larger K-size silica crucible made by DFC Ceramics™ of Canon City, Colorado. Sufficient filter-grade sand was added to the bottom of the silica crucible to prevent the alumina crucible from touching the silica crucible sidewall. In the event of breakage, the melt would be retained in the secondary crucible, thereby protecting the furnace. Two furnaces were used to prepare the glasses. The main glass melting furnace was a Model DT-31-12 bottom loading furnace made by Deltech, Inc. of Denver, Colorado. The maximum design temperature was 1704°C. The interior

workspace could accommodate a maximum work piece size of 292 mm in diameter and 292 mm high. A Lindberg/Blue-M Model 51894 laboratory box furnace used for preheating and annealing was made by Lindberg, Inc. of Watertown, Wisconsin.

The nested crucibles were preheated in the Blue-M furnace using a ramp rate of 3°C per minute to a temperature of 800°C in order to decrease the possibility of cracking the alumina crucibles due to thermal shock when the crucibles were subsequently transferred to the Deltech furnace at 1370°C for melting. Due to alumina crucible-furnace size restrictions, all of the mixed powder would not initially fit in the crucible. Powder was added four to eight times at fifteen minute intervals as the powder fused and decreased in volume. After the last powder addition, the melt was left at temperature for 1.25 hours to allow the melt to reach homogeneity. The melt was then quenched on a 19 mm thick type 304 stainless steel plate and after cooling it was stored in a plastic container.

To ensure homogeneity the glasses were ground in a Thomas-Wiley™ (Model 4) laboratory mill and sieved through a 35 mesh screen. The glass particles too large to go through the sieve were reground in a Tekmar mill until they passed the sieving criteria. Each of the powdered glasses was stored in a separate plastic container.

Next, approximately 300 g of the powdered glass was remelted in a 95% platinum/5% gold alloy crucible (for its release qualities) at 1370°C in order to manufacture the required samples. The melt was held at 1370°C for one hour prior to casting. The required samples consisted of XRF disks and constant surface area forms which would be used for the Toxicity Characteristic Leaching Procedure (TCLP) test, the Product Consistency Test (PCT), the XRD evaluation, and the archive samples. The constant surface area forms required milling before being used for PCT and XRD.

Two waste glass forms were produced with one being for XRF analysis and the other form, a constant surface area pellet, being used for the remainder of the tests performed for each of the glasses. Significant thought was given as to whether it would be preferable to pour the forms for XRF into graphite or platinum alloy molds. The

advantage of a platinum mold is that this type of mold produces a bottom surface that is ready for presentation to the XRF with no other surface preparation required. It also provides easy release from the mold. A study was carried out during the course of the project, to compare the XRF results from disks cast into platinum and graphite molds both made by SPEX Industries, Inc. of Edison, NJ. The study suggested that the surface of the disk from the graphite mold was of sufficient flatness and smoothness so as to generate good precision data. This was the result from multiple runs in the XRF. The results of this study also suggested that the increased costs of platinum molds were not justifiable. The high purity graphite molds for the XRF disks were 40 mm inside diameter at the bottom. They had slightly tapered sides to facilitate disk removal after cooling. The height of the molds was approximately 35 mm.

The second form for the pellets was also poured into graphite molds. These molds were prepared from blocks of high-purity graphite. The blocks measured 50x50x100 mm. Four rows of eight holes each (~9 mm in diameter by ~9 mm deep) were drilled as a set into two opposing longitudinal sides of the block, two sets per block. It was necessary to drill four blocks during the course of the research. Two blocks were used until they were worn down through oxidation and cleaning.

For each composition the graphite molds were preheated in the Blue-M furnace at 450°C for about fifteen minutes prior to casting in order to prevent the glass forms from cracking due to thermal shock. Observation suggested that longer heating of the molds caused an unacceptable oxidation layer to form on the graphite surfaces.

Two XRF disks approximately 10 mm thick were poured into two of the graphite molds. This thickness was chosen to ensure that no x-rays would pass completely through the sample.

After reheating the melt for three to five minutes, the molten glass was cast into constant surface area forms. A stainless steel plate was used to press the molten glass into the holes.

After the melt was again reheated for three to five minutes, the last two XRF disks were cast. After each set of samples was made, the molds were carefully cleaned using cheesecloth and Q-tips to remove any oxidized graphite.

After casting, all samples were annealed in the Blue-M furnace at 450°C for 40 minutes. The samples were then removed and allowed to cool to room temperature. Annealing relieved internal stresses and allowed the forms to be handled and polished with less chance of shattering.

After annealing and cooling, the disks were carefully labeled *A*, *B*, *C*, and *D* in the order that they were cast.

The glasses were polished using SiC paper on a Buehler polishing wheel to one mesh size higher than the final analyzed surface finish. Next, the glass was carefully abraded manually using a fresh sheet of the final 600 grit paper grade, first in one direction, then perpendicular to the original direction. This insured a reproducible finish with the correct number of scratches per inch.

After annealing and cooling, the constant surface area forms to be used for TCLP were sieved through a 9.5 mm screen in order to comply with EPA sample size requirements for TCLP. A TCLP sample with a constant surface area should provide more consistent results. After milling, constant surface area forms were also used for the PCT (Jantzen *et al.*, 1987), redox, and QCA analyses.

For these specific tests, the forms were ground into the appropriate particle size for the associated analysis.

In order to determine the effect of devitrification on the XRF intensity data, the *B* disk from each set was subsequently reheated to promote devitrification. This was carried out by heating the disks in the Blue-M furnace at a ramp rate of 5°C per minute to a temperature of 600°C for a duration of eight hours. The furnace was then ramped down to room temperature at a rate of 100°C per minute and the samples were allowed to cool

to room temperature. The XRF intensities collected from the *B* were compared to the *A* and *C* disks.

In conclusion, the sample types and quantities required for each composition point are delineated in Table VII.

Table VII. Samples Specifications

Sample Type Waste	Waste Form	Number &/or Weight (in gms) of Samples	Analysis
XRF Disks	40 mm dia. disk	4 (~120 g total)	XRF
TCLP Forms	9 mm X 9.5 mm pellets	30 pellets (~50 g total)	TCLP
TCLP Forms	9 mm X 9.5 mm pellets	~25 g	PCT. QCA, redox
TCLP Forms	9 mm X 9.5 mm pellets	~10 g	XRD
TCLP Forms	9 mm X 9.5 mm pellets	variable	Archive

Glass Analysis

Qualitative Chemical Analysis By Wet Chemical Methods

The elemental composition of six of the glasses was determined by Corning Environmental Laboratory Services (CELs) of Corning, New York. Analysis by CELs used hot HF dissolution for determination of Na_2O; cold HF dissolution for determination of B_2O_3; and alkali fusion dissolution for determination of the remainder of the oxides. After digestion, the digestate was analyzed by flame emission spectroscopy for Na_2O and ICPES for the balance of the oxides. Additionally, instrument calibration was carried out with standards with compositions individually tailored to be similar to the digestate to be analyzed. This procedure, called calibration with matrix matched standards, provided greater analytical accuracy.

Qualitative Chemical Analysis By XRF

The XRF analysis of the disks was performed at WSRC with a Rigaku Model 3271 wavelength-dispersive XRF spectrometer using 30 mm sample apertures and the instrument conditions listed in Table VIII. All of the disks were initially analyzed just for intensity data. The next phase was to pick which glasses would be included in the XRF study. This determination was based on a comparison of the intensity data. If all the elemental intensities for disks *A*, *C*, and *D* were statistically the same, the glass was deemed to be homogeneous. The intensity data were also used to compare the devitrified *B* disk with the *A* and *C* disks of the same set to determine if devitrification would impact XRF analysis of the elemental composition. The data from this study appear in Table XII.

Table VIII. XRF Instrument Parameters[a]

Element Line	Crystal	Detector[e]	Angle, 2θ	Collimator
B K_α	RX70[b]	PC	50.060	Coarse
Na K_α	RX35[c]	PC	26.175	Coarse
Al K_α	PET	PC	144.965	Coarse
Si K_α	RX4[d]	PC	144.650	Coarse
Ca K_α	LiF(200)	PC	113.200	Coarse
Fe K_α	LiF(200)	PC	57.570	Coarse
Ni K_α	LiF(200)	PC	48.705	Coarse
Ba L_α	LiF(200)	PC	87.350	Fine
Pb L_α	LiF(200)	SC	33.965	Coarse

[a]All elements were analyzed at 50kV, 50mA under vacuum.
[b]160 Å Mo-B4C multilayer crystal.
[c]60 Å W-Si multilayer crystal.
[d]45 Å W-Si multilayer crystal.
[e]PC = Flow Proportional Counter; SC = Scintillation Counter.

Next, the six samples analyzed by CELs were used as XRF analysis standards, with the Rigaku fundamental parameters (FP) program, to predict the elemental composition of the entire space. This was accomplished by using only the *A* disk from each of the disk sets that were determined to be homogeneous and running them in the XRF. Seven runs were made once with each of the six individual standards; and, then a last time using all six of the standards. After each of the runs, the elemental composition of each point in the entire compositional space was calculated using the FP program. The B_2O_3 content was determined by difference due to the difficulty in quantifying such a low atomic number element on the XRF.

Toxicity Characteristic Leaching Procedure Analysis

TCLP was performed on the constant surface area TCLP pellets at the Westinghouse Savannah River Company (WSRC). The data from this analysis are presented in graphical form in Appendix B in Tables B-III through B-X and in Table B-I.

Product Consistency Test Analysis

PCT analysis (Jantzen *et al.*, 1987) was performed using the glass samples originally cast into TCLP pellets and then further milled to the size appropriate for this test. A brief description of the test follows. Crushed glass of 100-200 mesh was immersed in ASTM Type I water for 7 days at 90°C. The volume of solution was 10 mL/g of washed glass. The leachate was filtered to remove colloidal and/or particulate material. The leachates were then analyzed to determine pH and elemental composition. The release of an element normalized by the weight fraction presence of the element in the composition is given by equation (3) in mg/L of glass in the leachate.

$$NRi = \frac{Ci}{Fi} \qquad (3)$$

where NR_i is the normalized release of the *i*th element in mg/L,

C_i = the concentration of the element in the leachate in mg/L, and

F_i = the weight fraction of the element in the glass.

In this thesis, NR_i is reported as the $\log_{10}$ NR. It should be noted that normalized release can be reported in several different units (Jantzen *et al.*, 1987).

Iron Redox Analysis

This analysis was performed by WSRC using a colorimetric method developed by Baumann (Baumann, 1987). The data from this analysis are located in Table A-XXXI.

X-Ray Diffraction Analysis

The XRD analysis for crystallinity in a selection of the glasses within the compositional space was performed at Clemson University with an XDS 2000 made by Scintag, Inc., of Sunnyvale, CA. using a side window x-ray tube with a nitrogen cooled scintillation detector. Comments on this preliminary study are located in in the Appendix in Table A-XXXII.

CHAPTER V

RESULTS

This chapter presents the results from the laboratory studies conducted to determine if XRF can be effectively utilized as a process control tool for the elemental analysis of waste glass. The results from TCLP, PCT, and redox are also included.

Qualitative Chemical Analysis by Wet Chemical Methods

The QCA as determined by wet chemical analysis by CELs for glasses 2MMM and 2HHH are compared with the target compositions in Table IX. The compositions of all the glasses are given in the Appendix in Table A-III.

Table IX. CELs Analysis versus Target for Elemental Composition

2MMM	CELs (Wt %)	Target (Wt %)	Difference (Wt %)	2HHH	CELs (Wt %)	Target (Wt %)	Difference (Wt %)
Al_2O_3	7.71	7.30	0.41	Al_2O_3	14.80	14.38	0.42
B_2O_3	4.31	4.60	0.29	B_2O_3	8.30	8.84	0.54
BaO	4.48	4.50	0.02	BaO	4.30	4.33	0.03
CaO	12.10	12.40	0.30	CaO	7.77	7.91	0.14
Fe_2O_3	4.85	4.70	0.05	Fe_2O_3	4.74	4.51	0.23
Na_2O	13.70	13.70	0.00	Na_2O	17.60	17.49	0.11
NiO	2.19	2.20	0.01	NiO	2.07	2.11	0.04
PbO	3.17	3.30	0.23	PbO	2.97	3.15	0.18
SiO_2	46.80	47.30	0.50	SiO_2	36.50	37.28	0.78
Total	99.31	100.00		Total	99.05	100.00	

Determination of Glass Homogeneity by XRF

Prior to the determination of the elemental composition of each glass with XRF, an experiment was carried out to determine if all the samples produced from a given melt were similar. This was especially important because the quantitative wet chemical analysis

was performed on the TCLP pellets while the XRF was performed on Disk *A*. If the melt was not homogeneous, the TCLP pellets may have a different composition from the XRF disks. This test of homogeneity was carried out by comparing the elemental intensities for each disk prepared for a given glass. Disks *A*, *C* and *D* were compared. Disk *B* was reheated to promote devitrification and was not used in this comparison.

After determining the XRF elemental intensities for each disk, the results were compared statistically to determine if they were similar. Any significant variation in elemental intensity for a given set of disks would signify that the melt might not be homogeneous. Table X shows the relative standard deviation in percent for the three elemental intensity values from disks *A*, *C* and *D*.

All of the glasses in Table X had RSDs of less than 1%, also reported by Resce (Resce *et al*, 1994). A value of 0.3% RSD was used as the maximum value to judge if the homogeneity of the glass was acceptable. The RSDs of most of the glasses measured in the tenths to hundredths of a percent. The glasses failing the homogeneity criteria were 1HHO, 3LHO, 4HOO, 4LHO, 6LHH, 6HOH, and 6HHH (not shown). Glasses missing from this table had cracked disks and could not be evaluated.

The error associated with XRF will be assumed to be a combination of the relative standard deviation of the *A*, *C*, and *D* for each of the elements for each of the glasses in the compositional space and the relative standard deviation associated with XRF precision. The XRF precision was determined by running one glass sample thirty times over an eight hour period. The resultant total error is the square root of the sum of the squares of these two individual errors. The results of this calculation are presented in Table XI.

Effect of Devitrification on XRF Intensities

An experiment performed to determine if devitrification impacts x-ray intensities. The *B* disks were reheated to promote devitrification by reheating at 450°C for 12 hours. The intensities from this disk were compared to the intensities from the two other disks

Table X. Relative Standard Deviations of Elemental Intensities from the Three Glass Disks to Determine Homogeneity (in percent RSD)

	Na	Pb	Ni	Fe	Ba	Ca	Si	Al
1LOO	1.738	0.907	0.121	0.551	0.852	0.637	0.634	1.468
1HOO	0.103	0.229	0.033	0.224	0.266	0.166	0.159	0.346
1LHO	0.140	0.102	0.022	0.115	0.040	0.003	0.050	0.081
1HHO	1.448	0.043	0.069	0.037	0.125	0.107	0.583	0.490
1LHH	0.172	0.178	0.064	0.040	0.198	0.116	0.231	0.034
2LOO	0.744	0.344	0.029	0.047	0.040	0.045	0.045	1.746
2HOO	1.527	0.245	0.096	0.232	0.086	0.069	0.263	1.824
2LHO	0.313	0.180	0.040	0.127	0.165	0.083	0.154	0.329
2HHO	0.875	0.104	0.043	0.197	0.123	0.058	0.140	2.857
2LOH	0.492	0.467	0.232	1.607	0.212	0.148	0.139	0.591
2HOH	0.986	0.351	0.137	0.061	0.213	0.205	0.245	0.234
2LHH	0.508	0.269	0.071	0.178	0.122	0.071	0.195	0.050
2HHH	0.446	0.355	0.096	0.006	0.256	0.119	0.258	0.129
3LOO	1.716	0.536	3.376	0.458	0.316	0.243	0.430	0.485
3HOO	0.516	0.290	0.653	0.390	0.433	0.159	0.683	1.035
3LHO	1.033	1.199	6.932	1.007	0.357	0.481	0.832	0.781
3HHO	0.171	0.286	1.464	0.143	0.071	0.027	0.068	0.238
3LHH	0.866	0.221	3.557	0.599	0.932	0.212	0.699	0.567
3HHH	0.665	0.650	4.086	0.706	0.836	0.393	1.583	0.450
4LOO	0.228	0.671	2.207	0.311	0.064	0.158	0.306	0.845
4HHO	0.816	0.410	1.099	0.143	0.242	0.134	0.787	0.227
6LOH	0.045	2.177	2.547	0.158	0.378	0.258	0.323	0.074
6LHH	1.376	2.077	8.305	3.456	0.666	0.723	1.790	1.603
MID1	0.929	0.162	0.036	0.039	0.100	0.011	0.215	0.121
MID2	1.142	0.065	0.095	0.120	0.123	0.073	0.278	0.180
MID3	0.322	0.573	0.082	0.088	0.070	0.071	0.230	0.153
MMOO	0.458	0.232	0.034	0.093	0.086	0.087	0.190	1.334
MMHO	0.478	0.164	0.132	0.043	0.133	0.049	0.178	0.271
1,2MMH	0.190	0.518	0.062	0.115	0.093	0.069	0.268	0.121
2MMM	0.132	0.206	0.058	0.281	0.044	0.083	0.235	0.102
4MMM	0.424	0.627	2.514	0.832	0.128	0.250	0.593	0.039
3MMM	0.193	0.372	2.148	0.097	0.205	0.040	0.472	0.221
2HHOZ	0.339	0.120	0.036	0.137	0.722	0.124	0.385	0.297
2LOHZ	0.434	0.707	0.177	0.069	0.083	0.119	0.269	0.144

Table XI. Error Associated with Fundamental Parameter in Weight Percentages

	Na	Pb	Ni	Fe	Ba	Ca	Si	Al
Error - Disks	0.752	0.451	1.149	0.356	0.258	0.165	0.411	0.572
Precision Error	0.280	0.164	0.015	0.050	0.350	0.210	0.050	0.190
Total Error	0.802	0.480	1.149.	0.435	0.435	0.267	0.414	0.603

which were not reheated. It was assumed that Disk *B* had a greater extent of devitrification than the other two, therefore, any difference in intensities would reflect the effect of reheating. The values in the table were calculated as follows. The *A&C* value was determined by subtracting the *A* disk XRF intensity from the *C* disk intensity and dividing the result by the *A* intensity. This result is reported as a percentage difference in the x-ray intensities between the two disks of the same set for that element. The *A&C to B* value was determined by dividing the average of the *A* and *C* intensities minus the *B* intensity by the average of the *A* and *C* intensities. This result is reported as a percentage. This provides a measure of how different the XRF intensities from the devitrified *B* disks were from the XRF intensities of the *A* and *C* disks. The results from this experiment are reported in Table XII.

The table shows that a difference in the XRF intensities due to devitrification is a consideration for most of the glasses. The 1-Space glasses, extremely low Si glasses, produced the least acceptable results from this experiment. The glasses missing from this table had either all cracked disks or a cracked *B* disk and could not be evaluated.

QCA by XRF from Fundamental Parameters (FP)

The XRF FP analysis was performed on all 43 glasses using two different standards. The first analysis utilized the low iron 2MMM glass standard and the second utilized the high iron 3MMM glass standard. Disk A from each of the 43 glasses was tested. The results are presented in the Appendix in Tables A-IV and A-V. The determination of how well these results correlated with the analysis by wet chemical methods followed by ICPES and/or AA (hereinafter referred to as ICP) is presented here. Six glasses were examined. These 6 glasses analyzed by CELs are summarized in Table XIII. Tables XIV and XV present the results of a comparison of the CELs analysis with the XRF fundamental parameters analysis.

Table XII. Effect of Devitrification on Elemental Intensities
(in Percent Difference)

Glass	Disks	Na	Pb	Ni	Fe	Ba	Ca	Si	Al
1LOO	*A&C*	0.50	-1.58	-0.25	-0.78	-2.15	1.18	1.10	-2.64
	A&C to B	-4.13	-0.56	0.43	-0.39	0.94	1.21	-0.24	-1.12
1HOO	*A&C*	0.21	0.55	0.07	-0.01	0.58	-0.25	0.23	0.66
	A&C to B	-8.28	14.43	-1.06	-2.75	1.10	-1.99	-1.17	1.88
1LHO	*A&C*	-0.34	0.19	0.05	-0.10	0.03	0.00	0.10	-0.20
	A&C to B	-11.01	29.41	3.39	-9.77	-4.62	-5.46	-5.63	1.86
1HHO	*A&C*	-0.15	-0.15	-0.06	-0.08	-0.24	-0.02	-0.08	-0.20
	A&C to B	-7.18	9.57	3.44	-4.75	3.00	-2.91	-5.08	1.86
2LOO	*A&C*	1.36	-0.11	-0.07	-0.08	-0.06	0.01	-0.11	-0.46
	A&C to B	-1.97	-0.22	1.51	-0.67	-1.68	1.21	0.59	1.39
2HOO	*A&C*	-0.58	-0.57	0.03	0.05	0.11	-0.07	-0.08	-2.26
	A&C to B	-0.07	-0.04	-0.08	-0.04	0.24	-0.09	-0.01	-0.20
2LHO	*A&C*	-0.63	0.44	0.08	-0.23	0.20	-0.13	-0.36	-0.33
	A&C to B	-0.13	0.07	-0.06	-0.02	-0.02	0.00	-0.88	0.12
2HHO	*A&C*	-1.74	-0.15	-0.03	-0.46	-0.11	-0.14	-0.28	5.82
	A&C to B	0.91	0.16	-0.04	0.21	0.01	-0.05	-0.02	3.47
2LOH	*A&C*	0.71	-1.08	-0.49	3.76	0.34	-0.10	-0.30	-1.32
	A&C to B	-0.14	0.02	-0.22	-0.66	-0.24	-0.11	0.56	0.05
2HOH	*A&C*	-1.95	0.59	-0.02	-0.13	-0.42	-0.48	-0.40	-0.51
	A&C to B	1.05	0.68	-0.14	-0.11	-0.13	0.10	0.65	0.01
2LHH	*A&C*	0.43	0.36	0.07	0.34	-0.17	-0.07	-0.10	-0.08
	A&C to B	-0.74	0.11	-0.11	-0.08	0.28	-0.02	-0.28	0.33
3LOO	*A&C*	-0.95	-1.66	6.76	0.71	0.32	-0.26	-0.68	-0.10
	A&C to B	-5.71	0.62	-2.07	-0.27	0.38	-0.18	-1.98	-2.98
3HOO	*A&C*	-0.99	0.66	0.64	0.58	0.37	0.04	-1.37	-1.49
	A&C to B	0.97	0.87	-0.96	0.27	0.04	0.39	-0.05	0.93
3LHO	*A&C*	-2.41	-3.05	15.00	1.70	-0.70	-1.04	-1.25	-1.76
	A&C to B	-0.28	1.80	-8.83	-0.73	0.31	0.39	-0.08	-0.78
3HHO	*A&C*	-0.34	0.57	-2.97	-0.29	0.14	0.05	-0.14	0.48
	A&C to B	-0.52	4.17	-2.07	-1.41	7.68	-2.92	-3.24	3.79
3HHH	*A&C*	6.21	-0.85	8.52	0.60	-1.62	0.00	0.00	0.00
	A&C to B	-2.76	0.47	3.27	1.24	0.02	1.02	0.45	0.23
4LOO	*A&C*	0.55	0.32	1.50	0.15	0.10	0.20	-0.75	0.67
	A&C to B	1.24	0.39	-0.47	0.06	-0.33	-0.10	-0.59	-0.13
4HOO	*A&C*	2.24	-4.87	-3.27	-1.25	-0.13	-1.39	3.22	2.84
	A&C to B	5.99	-0.86	0.96	0.48	1.40	0.33	2.12	2.66
4LHO	*A&C*	2.24	-4.87	-3.27	-1.25	-0.13	-1.39	3.22	2.84
	A&C to B	5.99	-0.86	0.96	0.48	1.40	0.33	2.12	2.66
4HHO	*A&C*	1.18	0.35	2.34	0.34	0.14	0.06	-1.90	-0.51
	A&C to B	-2.27	1.02	1.25	0.05	0.27	-0.23	-0.07	-1.67

Table XII. (Continued)

Glass	Disks	Na	Pb	Ni	Fe	Ba	Ca	Si	Al
6LOH	*A&C*	0.09	-4.45	-5.23	0.32	0.75	0.52	0.64	0.15
	A&C to B	-9.91	5.11	-4.01	10.25	0.04	0.55	3.32	0.31
6HOH	*A&C*	0.56	-5.26	-0.46	-2.23	0.85	1.11	1.58	1.64
	A&C to B	-2.28	-4.02	0.27	0.65	0.31	0.28	2.12	2.94
6LHH	*A&C*	2.91	3.93	-16.52	-6.01	1.44	1.55	2.55	2.89
	A&C to B	-2.27	-1.68	7.04	3.09	-0.43	-0.67	-0.79	2.71
6HHH	*A&C*	0.60	0.75	-2.02	-0.12	-0.11	-0.20	-0.55	0.05
	A&C to B	-3.13	0.73	-0.21	0.42	0.25	0.15	0.62	3.70
MID1	*A&C*	1.21	-0.07	0.05	0.02	-0.07	-0.02	-0.16	-0.16
	A&C to B	-9.84	1.38	0.33	0.39	7.82	-3.01	-4.70	-7.83
MID2	*A&C*	1.85	-0.13	-0.21	0.08	0.14	0.04	-0.09	-0.28
	A&C to B	-6.97	5.68	0.17	-0.64	9.39	-3.16	-5.13	-8.58
MID3	*A&C*	-0.31	0.89	-0.19	-0.15	-0.17	-0.16	-0.42	-0.20
	A&C to B	-1.47	-0.10	0.52	0.13	0.19	-0.06	0.90	-0.76
MMOO	*A&C*	-1.07	0.33	-0.06	-0.17	-0.03	0.18	-0.23	1.74
	A&C to B	0.58	0.24	0.08	0.04	-0.05	-0.06	-0.50	1.69
MMHO	*A&C*	-0.94	0.40	0.27	0.02	-0.17	-0.10	-0.39	0.44
	A&C to B	-0.31	-0.28	0.27	-0.06	0.05	0.04	0.46	-1.87
1,2MMH	*A&C*	0.39	0.71	-0.17	-0.18	-0.17	-0.05	-0.71	0.05
	A&C to B	-0.32	-1.55	-0.03	0.20	0.13	0.17	0.27	-0.02
2MMM	*A&C*	0.18	0.25	-0.07	-0.57	0.07	-0.19	0.12	-0.01
	A&C to B	-0.02	0.00	0.12	-0.03	0.09	0.02	0.59	0.05
4MMM	*A&C*	-0.09	0.69	0.12	-0.28	-0.01	0.14	-0.79	0.07
	A&C to B	3.36	-0.27	-0.52	-0.23	-0.12	-0.17	-0.41	-0.90
2HHOZ	*A&C*	0.78	0.27	-0.09	-0.02	-1.51	-0.30	0.33	-0.63
	A&C to B	-0.12	-0.01	0.22	-0.02	0.88	0.05	0.65	0.10
2LOHZ	*A&C*	0.78	0.44	-0.34	0.00	0.01	0.14	0.02	-0.06
	A&C to B	-0.29	-1.48	0.14	0.07	0.29	0.20	0.07	0.06

Table XIII. CELs Analysis of the CELs Glasses (in wt%)

	2MMM	2HHH	MID1	MMHO	1,2MMH	3MMM
Al_2O_3	7.71	14.80	6.77	1.18	14.50	8.11
B_2O_3	4.31	8.30	2.83	6.32	3.54	2.02
BaO	4.48	4.30	3.98	4.19	4.29	3.41
CaO	12.10	7.77	12.80	13.80	15.50	12.70
Fe_2O_3	4.85	4.74	20.10	19.90	4.80	32.00
Na_2O	13.70	17.60	14.80	15.30	17.90	15.10
NiO	2.19	2.07	1.90	2.00	2.07	1.65
PbO	3.17	2.97	2.77	2.93	2.89	2.37
SiO_2	46.80	36.50	31.40	34.20	32.50	20.90

Table XIV. Comparison of the CELs Analysis with Fundamental Parameters Analysis. The 3MMM standard is used in the analysis of the six CELs Glasses. The values are in oxide weight %.

	Na_2O	Al_2O_3	BaO	CaO	Fe_2O_3	NiO	PbO	SiO_2	B_2O_3
2MMM									
FP	13.87	7.68	4.45	12.08	5.08	2.26	3.23	46.52	3.09
CELs	13.70	7.71	4.48	12.10	4.85	2.19	3.17	46.80	4.31
Difference	**0.17**	**(0.03)**	**(0.03)**	**(0.02)**	**0.23**	**0.07**	**0.06**	**(0.28)**	**(1.22)**
3MMM									
FP	15.14	8.14	3.42	12.80	32.26	1.67	2.40	21.18	1.25
CELs	15.10	8.11	3.41	12.70	32.00	1.65	2.37	20.90	2.02
Difference	**0.04**	**0.03**	**0.01**	**0.10**	**0.26**	**0.02**	**0.03**	**0.28**	**0.77**
1,2MMH									
FP	17.89	14.69	4.29	15.65	5.09	2.17	2.97	32.75	2.78
CELs	17.90	14.50	4.29	15.50	4.80	2.07	2.89	32.50	3.54
Difference	**(0.01)**	**0.19**	**0.0**	**0.15**	**0.29**	**0.10**	**0.08**	**0.25**	**0.76**
MMHO									
FP	15.37	1.18	4.18	13.78	20.15	2.04	2.96	34.07	4.54
CELs	15.30	1.18	4.19	13.80	19.90	2.00	2.93	34.20	6.32
Difference	**0.07**	**0.0**	**(0.01)**	**(0.02)**	**0.25**	**0.04**	**0.03**	**(0.13)**	**(1.78)**
MID1									
FP	14.73	6.88	4.03	13.05	20.90	1.99	2.85	31.97	1.86
CELs	14.80	6.77	3.98	12.80	20.10	1.90	2.77	31.40	2.83
Difference	**(0.07)**	**0.11**	**0.05**	**0.25**	**0.80**	**0.09**	**0.08**	**0.57**	**0.97**
2HHH									
FP	17.68	14.76	4.36	7.84	5.04	2.18	3.08	36.74	6.60
CELs	17.60	14.80	4.30	7.77	4.74	2.07	2.97	36.50	8.30
Difference	**0.08**	**(0.04)**	**0.06**	**0.07**	**0.30**	**0.11**	**0.11**	**0.24**	**1.70**

- The parentheses around the *Difference* value indicates that the *CELs* value was larger than the *FP* value.

Table XV. Comparison of the CELs Analysis with Fundamental Parameters Analysis. The 2MMM standard is used in the analysis of the six CELs Glasses. The values are in oxide weight %.

	Na_2O	Al_2O_3	BaO	CaO	Fe_2O_3	NiO	PbO	SiO_2	B_2O_3
2MMM									
FP	13.71	7.74	4.50	12.15	4.89	2.20	3.19	47.08	3.84
CELs	13.70	7.71	4.48	12.10	4.85	2.19	3.17	46.80	4.31
Difference	**0.01**	**0.03**	**0.02**	**0.05**	**0.04**	**0.01**	**0.02**	**0.28**	**0.47**
3MMM									
FP	14.77	7.95	3.40	12.53	30.29	1.56	2.27	20.36	5.91
CELs	15.10	8.11	3.41	12.70	32.00	1.65	2.37	20.90	2.02
Difference	**(0.33)**	**(0.16)**	**(0.01)**	**(0.17)**	**(1.71)**	**(0.09)**	**(0.10)**	**(0.54)**	**3.89**
1,2MMH									
FP	17.85	14.64	4.33	15.70	4.86	2.11	2.94	32.76	4.12
CELs	17.90	14.50	4.29	15.50	4.80	2.07	2.89	32.50	5.55
Difference	**(0.05)**	**0.14**	**0.04**	**0.20**	**0.06**	**0.04**	**0.05**	**0.26**	**(1.43)**
MMHO									
FP	15.18	1.17	4.17	13.67	19.17	1.94	2.87	33.87	7.78
CELs	15.30	1.18	4.19	13.80	19.90	2.00	2.93	34.20	6.50
Difference	**(0.12)**	**(0.01)**	**(0.02)**	**(0.13)**	**(0.13)**	**(0.06)**	**(0.04)**	**(0.33)**	**0.77**
MID1									
FP	14.57	6.77	4.03	12.95	19.91	1.90	2.78	31.67	4.74
CELs	14.80	6.77	3.98	12.80	20.10	1.90	2.77	31.40	5.48
Difference	**(0.23)**	**0.00**	**0.05**	**0.15**	**(0.19)**	**0.00**	**0.01**	**0.27**	**(0.74)**
2HHH									
FP	17.55	14.78	4.37	7.83	4.83	2.11	3.04	36.75	8.06
CELs	17.60	14.80	4.30	7.77	4.74	2.07	2.97	36.50	9.25
Difference	**(0.05)**	**(0.02)**	**0.07**	**0.06**	**0.09**	**0.04**	**0.07**	**0.25**	**(1.19)**

The parentheses around the *Difference* value indicates that the *CELs* value was larger than the *FP* value.

Because the XRF analysis was based on these glasses, for convenience, the six glasses analyzed by CELs were grouped together and defined as the CELs Glasses. These glasses appear in Table XIII. Two cases are presented with the first using the high iron 3MMM standard with fundamental parameters to predict the CELs Glasses and the second using the low iron 2MMM standard with fundamental parameters to predict the CELs Glasses. As an example, the first section of Table XIV shows the prediction for the 2MMM glass using fundamental parameters with the 3MMM standard. The first line contains the FP evaluated elemental weight percent data and the second line contains the CELs elemental weight percent data of this glass. The third line reflects the difference between the weight percents from FP and CELs.

In most cases there is a very small difference between the FP elemental weight percentages and the CELs elemental weight percentages. The results appear in Tables XIV and XV.

The results from the following topics appear in the associated appendices; Toxicity Characteristic Leaching Procedure (TCLP)—Appendix in B; Product Consistency Test (PCT)—Appendix C; Iron Redox Analysis—Appendix D; X-Ray Diffraction Analysis—Appendix E; and Glass Sampling from the Pilot-Scale Melter—Appendix F.

CHAPTER VI

DISCUSSION

This chapter discusses the results from the laboratory studies conducted to determine if XRF can be effectively utilized as a process control tool for the elemental analysis of waste glass. Also included is a discussion of the results from QCA, TCLP, PCT, and redox tests.

Qualitative Chemical Analysis by Wet Chemical Methods

Because of the extensive use of AA/ICPES as an analysis tool in industry, the process is very well characterized and understood (Ryan and Radford, 1987). Also, these ICP results were obtained from CELs. Effort was made by CELs to ensure that the wet chemistry analysis was as accurate as possible as it was the basis for evaluating the performance of the XRF FP program. The analyses were performed using matrix-matched standards to obtain the most accurate results by eliminating as many matrix effects as possible. One measure of the accuracy of an ICP analysis is how close the sum of the individual elemental weight percentages approaches 100 wt%. Half of the CELs analyses performed totaled in excess of 99 wt% for the sum of the weight percentages of the elemental compositions and all of the analyses totaled above 97 wt%.

The main goal of the thesis was to determine if XRF could be used as a process control tool using FP calculated elemental composition. The XRF FP results were compared to ICP analysis of the same glasses.

The error in precision associated with ICP is assumed to be +/- 1.5 percent (Ryan and Radford, 1987).

Determination of Glass Homogeneity by XRF

Glass homogeneity was one of the prerequisites of this research. As previously described, analytical accuracy of XRF results is very dependent on sample homogeneity. In order to evaluate this concern, an experiment was carried out to determine if all the samples produced from a given melt were similar. This was especially important because the quantitative wet chemical analysis was performed on the TCLP pellets while the XRF was performed on Disk *A*. XRF Disks *A* and *B* were cast first and then after reheat time, the TCLP pellets were cast. If the melt was not homogeneous, the TCLP pellets which were poured in the second casting could have a different composition from the XRF disks. This test of homogeneity was carried out by comparing the elemental intensities for disks which were cast before and after the TCLP pellets. Disks *A*, *C*, and *D* were compared.

After determining the elemental intensities for each disk, the results were compared statistically to determine if they were similar. Any significant variation in elemental intensity for a given set of disks would signify that the melt was probably not homogeneous. Table X of Chapter V shows the relative standard deviation in percent for the three elemental intensity values from Disks *A*, *C*, and *D*.

In this thesis, a 1% RSD was considered to be good. All of the compositional space glasses had RSDs of less than 1%. To remain on the conservative side, a value of 0.3% RSD was chosen as the maximum value to judge if the homogeneity of the glass was acceptable. Of the 43 glasses, the nine which failed the homogeneity criteria were 1HHO, 3LHO, 4HOO, 4LHO, 5HOO, 6HOO, 6LHH, 6HOH, and 6HHH. Several other glasses were not included because their disks broke. Approximately 67% of the original compositional space glasses were judged adequate by the criteria of homogeneity. One conclusions may be drawn from this section. This conclusion is that the majority of the glasses in the compositional space were homogeneous.

Effect of Devitrification on XRF Intensities

The XRF FP method of quantifying elemental composition assumes that the glass samples have little or no crystallinity. However, depending upon the cooling rate, many waste glasses are subject to devitrification. An effort has been made, therefore, to determine what effect devitrification has on XRF intensities. It was decided to reheat one disk of each set as described in the experimental procedures in Chapter IV in order to promote devitrification. The intensities from this disk were then compared to the other disks. Table XII of Chapter V contains the results of this experiment.

An inspection of the data was performed, comparing the *A&C* data with the associated *A&C to B* data. If the *A&C to B* data was in excess of 4% greater than the *A&C* data then reheating was assumed to have had an effect on the elemental XRF intensities. The table suggests that reheating does effect the XRF intensities of most of the glasses, with the exception that there was no affect on the 2-Space glasses. This may have been due to the fact that the 2-Space glasses did not devitrify upon reheating. Although the elemental interactions in the melt are much more complex, the negative impact of devitrification approximately followed the Ca/Na levels in the glass. Reheating the 1-Space glasses appeared to have the greatest effect on XRF intensities. As a subspace, they were extremely low Si and high Ca/Na glasses that probably would not be deliberately produced in a vitrification operation. At the other end of the spectrum, the 2-Space glasses with lower Ca/Na levels and the highest Si levels had the least problems with devitrification in this experiment. The 4-Space and then the 3-Space, respectively, were the next two spaces least effected by devitrification. In conclusion, the XRF intensities are affected when the sample is reheated for 8 hours at 600°C. Thus it appears that devitrification does affect XRF analysis. It would be of interest to perform XRD on the reheated samples to further support this conclusion.

QCA by XRF from Fundamental Parameters

Tables XIV and XV present the results of a comparison of the CELs analysis with the XRF FP analysis. The specific glasses included are reported in Table XIII. Two cases are presented with the first using the 3MMM standard with FP to predict the CELs Glasses and the second using the 2MMM standard with FP to predict the CELs Glasses. As an example, the first section of this table shows the prediction for the 2MMM glass with the 3MMM standard. The first row contains the FP data and the second row contains the CELs analysis data of this glass. The third row reflects the difference between the weight percents from FP and CELs. B_2O_3 composition for each glass was determined by difference.

Tables XIV and XV show that in most cases there is a very small difference between the FP and the CELs values for the oxide weight percentages. These differences are within experimental error. The conclusion to be made from these data is that XRF FP does correlate with the elemental compositions as determined by ICP (CELs) over the entire range of the composition space.

Comparison of the Use of Two Standards with FP

This section provides additional evidence to support the main objective of this research that XRF can be effectively utilized as a process control tool for the elemental analysis of waste glass. The statistical correlation between the XRF FP results and the wet chemical analysis by CELs (specifically ICP) is examined in this section. This correlation meets the requirements of the third experimental objective.

Two cases were considered to evaluate FP for prediction of the composition of the glasses. The first case uses the single standard 3MMM to predict the CELs Glasses. In the next case, the 2MMM standard was used to predict the CELs Glasses. Both of the cases were then compared. In each case, linear regression was used to fit the data. The linear regression best fit line was forced through the origin. The slope, R^2 value, and the

standard error are recorded in Table XVI for each of the cases. The ideal line would have a slope of one. If the data points were to fall on this line, it would indicate that the XRF FP value for the associated point was exactly equal to the wet chemistry QCA value. Deviation would indicate that XRF did not predict the elemental composition. The line of data labeled *"Difference"* reflects the absolute difference between the ideal slope and the slope from the linear regression data fit. The data in this table shows that the XRF FP program does an excellent job of predicting the elemental compositions of the samples. For the 3MMM standard predicting the CELs Glasses, discounting the B_2O_3 which was evaluated by difference, all the rest of the oxides were predicted with regressed slopes that match the ideal slope to the second or third decimal place. The associated R^2 and standard errors support the conclusion that the XRF FP prediction matches the ICP analysis. Overall, the XRF FP analysis with the 2MMM standard does not correlate with the ICP results as well as the 3MMM standard predictions. The 3MMM standard may have done a slightly better job because the iron content of the standard was higher than that of the glasses being analyzed (Criss, 1994; Jurgensen, 1994). The conclusion remains, however, that XRF with a FP program can be used very successfully to analyze waste glass.

Discussion of the results from the following topics appear in the associated appendices; Toxicity Characteristic Leaching Procedure Analysis—Appendix B; Product Consistency Test Analysis—Appendix C; Iron Redox Analysis—Appendix D; X-Ray Diffraction Analysis—Appendix E; Glass Sampling from a Pilot-Scale Melter—Appendix F; and Miscellaneous—Appendix G.

Table XVI. Linear Regression Analysis of the CELs Glasses. Linear regression was used to fit the data from the analyses using the 3MMM standard and the 2MMM standard to ICP analysis.

	Na_2O	Al_2O_3	BaO	CaO	Fe_2O_3	NiO	PbO	SiO_2	B_2O_3
3MMM standard predicting the CELs Glasses									
Slope	1.0028	1.0048	1.0027	1.0070	1.0180	1.0360	1.0230	1.0030	1.0650
Difference	0.0028	0.0048	0.0027	0.0070	0.0180	0.0360	0.0230	0.0030	0.0650
R^2	0.9907	0.9997	0.9902	0.9908	0.9909	0.9709	0.9809	0.9980	0.8809
Std Error	0.0803	0.0871	0.0304	0.1002	0.2807	0.0301	0.0300	0.3310	0.6500
2MMM standard predicting the CELs Glasses									
Slope	0.992	1.0012	1.0061	1.0023	0.9620	0.9970	1.00096	1.0030	1.1140
Difference	0.008	0.0012	0.0061	0.0023	0.0380	0.0030	0.00004	0.0030	0.1140
R^2	0.994	0.9997	0.9921	0.9970	0.9990	0.9410	0.9600	0.9989	0.2206
Std Error	0.131	0.0906	0.0351	0.1408	0.3809	0.0506	0.0603	0.2709	1.9105

CHAPTER VII

CONCLUSIONS

The purpose of this study was to investigate x-ray fluorescence spectrometry analysis as a near real-time method to determine melter glass compositions. This project formulated and produced a range of glasses derived from wastewater treatment sludges associated with DOE sites.

Several analysis methods were applied to the investigation in order to obtain the necessary information for accomplishing the research objectives. Inductively coupled plasma emission spectrometry/atomic absorption was used to determine the elemental composition of the glasses. X-ray fluorescence spectrometry was also used to determine the elemental compositions of the glasses in order to make a comparison between these two methods. The toxicity characteristic leaching procedure and product consistency test were used to evaluate leaching for the glasses. X-ray diffraction and microscopy were used to characterize any crystallinity associated with the glasses. Redox was performed to characterize the redox state of the glasses. The data collected using these methods of analysis enabled the researcher to reach several conclusions with respect to the purpose of the investigation and the defined research objectives.

1. A rapid method was developed to sample molten glass and make disks for XRF spectrometric elemental analysis.

2. A significant decrease in compositional analysis time through the use of XRF spectrometry versus digestion with AA/ICPES analysis was demonstrated.

3. Good correlation was demonstrated between conventional wet chemistry digestion with AA/ICPES analysis with XRF analysis of the waste glasses.

4. A procedure was developed for making consistent constant surface area waste glass forms appropriate for Toxic Characteristic Leaching Procedure (TCLP) testing.

5. The leaching behavior of the glasses was evaluated with TCLP and PCT.

CHAPTER VIII

RECOMMENDATIONS

The following recommendations are submitted as suggestions for areas of further study:

1. Further determine what effect devitrification has on XRF analysis in order to more completely evaluate the impact of devitification on elemental analysis by XRF.

2. Model the correlation between PCT and glass composition in order to be able to predict glass durability based on the composition.

3. Model the correlation between TCLP and glass composition in order to be able to predict glass durability based on the composition.

4. Model the correlation between PCT and TCLP to compare the results from the two different tests and determined which method should be used to most correctly predict the durability of the glass.

5. Submit the rest of the glasses to Corning Environmental Laboratory Services for analysis and use these analyses to expand on the results from the current study of the compositional space with XRF.

6. Demonstrate that XRF will provide satisfactory analysis on actual low-level or mixed waste glass forms. It remains to be determined whether or not the presence of radionuclides will adversely affect XRF analysis.

APPENDICES

Appendix A

Compositional Space and Fundamental Parameters Analysis

The tables in this appendix present data related to the composition of the compositional space and data and plots related to the XRF evaluation of the compositional space by fundamental parameters.

Table A-I. Compositional Space (Target) - Oxides in Weight Percent

	SiO_2	CaO	Na_2O	Fe_2O_3	B_2O_3	Al_2O_3	BaO	NiO	PbO
1LOO	38.9%	29.4%	16.3%	4.9%	0.0%	0.0%	4.7%	2.3%	3.4%
1LHO	33.1%	29.2%	16.1%	4.9%	6.4%	0.0%	4.7%	2.3%	3.4%
1HOO	38.3%	14.5%	32.0%	4.9%	0.0%	0.0%	4.7%	2.3%	3.4%
1HHO	32.6%	14.4%	31.7%	4.8%	6.3%	0.0%	4.6%	2.2%	3.4%
2LOO	58.0%	17.2%	9.5%	4.9%	0.0%	0.0%	4.7%	2.3%	3.4%
2LHO	49.1%	17.0%	9.4%	4.8%	9.5%	0.0%	4.6%	2.3%	3.4%
2HOO	57.5%	8.5%	18.8%	4.9%	0.0%	0.0%	4.7%	2.3%	3.4%
2HHO	48.6%	8.4%	18.6%	4.8%	9.4%	0.0%	4.6%	2.2%	3.3%
3LOO	26.0%	19.4%	10.7%	35.5%	0.0%	0.0%	3.8%	1.8%	2.8%
3LHO	22.1%	19.3%	10.7%	35.3%	4.3%	0.0%	3.8%	1.8%	2.7%
3HOO	25.7%	9.6%	21.2%	35.2%	0.0%	0.0%	3.8%	1.8%	2.7%
3HHO	21.9%	9.5%	21.1%	34.9%	4.2%	0.0%	3.7%	1.8%	2.7%
4LOO	41.3%	9.6%	5.3%	35.3%	0.0%	0.0%	3.8%	1.8%	2.7%
4LHO	35.1%	9.6%	5.3%	35.0%	6.8%	0.0%	3.7%	1.8%	2.7%
4HOO	41.1%	4.8%	10.6%	35.1%	0.0%	0.0%	3.7%	1.8%	2.7%
4HHO	34.9%	4.8%	10.5%	34.8%	6.7%	0.0%	3.7%	1.8%	2.7%
1LOH	27.9%	27.6%	15.3%	4.6%	0.0%	14.8%	4.4%	2.2%	3.2%
1LHH	22.4%	27.4%	15.1%	4.6%	6.0%	14.7%	4.4%	2.1%	3.2%
1HOH	27.5%	13.6%	30.1%	4.6%	0.0%	14.6%	4.4%	2.1%	3.2%
1HHH	22.1%	13.5%	29.9%	4.5%	5.9%	14.4%	4.3%	2.1%	3.2%
2LOH	45.9%	16.2%	8.9%	4.6%	0.0%	14.7%	4.4%	2.2%	3.2%
2LHH	37.6%	16.0%	8.8%	4.5%	8.9%	14.5%	4.4%	2.1%	3.2%
2HOH	45.5%	8.0%	17.7%	4.6%	0.0%	14.6%	4.4%	2.1%	3.2%
2HHH	37.3%	7.9%	17.5%	4.5%	8.8%	14.4%	4.3%	2.1%	3.1%
3LOH	17.6%	18.4%	10.2%	33.8%	0.0%	12.0%	3.6%	1.8%	2.6%
3LHH	14.0%	18.3%	10.1%	33.6%	4.1%	11.9%	3.6%	1.7%	2.6%
3HOH	17.5%	9.1%	20.2%	33.4%	0.0%	11.9%	3.6%	1.7%	2.6%
3HHH	13.9%	9.1%	20.1%	33.3%	4.0%	11.8%	3.5%	1.7%	2.6%
6LOH	37.7%	12.0%	6.6%	22.0%	0.0%	13.0%	3.9%	1.9%	2.9%
6HOH	38.8%	6.3%	13.9%	19.0%	0.0%	13.2%	4.0%	1.9%	2.9%
6LHH	29.8%	11.2%	6.2%	24.7%	7.2%	12.6%	3.8%	1.8%	2.8%
6HHH	29.1%	5.4%	11.9%	26.0%	7.0%	12.4%	3.7%	1.8%	2.7%
MID1	32.1%	13.3%	14.7%	21.0%	3.2%	6.7%	4.0%	2.0%	2.9%
MID2	32.1%	13.3%	14.7%	21.0%	3.2%	6.7%	4.0%	2.0%	2.9%
MID3	32.1%	13.3%	14.7%	21.0%	3.2%	6.7%	4.0%	2.0%	2.9%

Table A-I. (Continued)

	SiO_2	CaO	Na_2O	Fe_2O_3	B_2O_3	Al_2O_3	BaO	NiO	PbO
MMOO	40.9%	14.1%	15.6%	20.1%	0.0%	0.0%	4.2%	2.1%	3.1%
MMHO	34.7%	14.0%	15.4%	19.9%	6.7%	0.0%	4.2%	2.0%	3.0%
2MMM	47.4%	12.4%	13.7%	4.7%	4.6%	7.3%	4.5%	2.2%	3.3%
3MMM	19.8%	14.1%	15.5%	34.4%	2.1%	5.9%	3.7%	1.8%	2.7%
4MMM	33.7%	7.0%	7.7%	34.2%	3.3%	5.9%	3.7%	1.8%	2.7%
1,2MMH	33.3%	16.3%	17.9%	4.6%	3.7%	14.6%	4.4%	2.1%	3.2%

Table A-II. Compositional Space (Target) - Oxides in Mole Percent

	Si	Ca	Na	Fe	B	Al	Ba	Ni	Pb
1LOO	42%	34%	17%	2%	0%	0%	2%	2%	1%
1LHO	36%	34%	17%	2%	6%	0%	2%	2%	1%
1HOO	42%	17%	34%	2%	0%	0%	2%	2%	1%
1HHO	36%	17%	34%	2%	6%	0%	2%	2%	1%
2LOO	63%	20%	10%	2%	0%	0%	2%	2%	1%
2LHO	54%	20%	10%	2%	9%	0%	2%	2%	1%
2HOO	63%	10%	20%	2%	0%	0%	2%	2%	1%
2HHO	54%	10%	20%	2%	9%	0%	2%	2%	1%
3LOO	35%	28%	14%	18%	0%	0%	2%	2%	1%
3LHO	30%	28%	14%	18%	5%	0%	2%	2%	1%
3HOO	35%	14%	28%	18%	0%	0%	2%	2%	1%
3HHO	30%	14%	28%	18%	5%	0%	2%	2%	1%
4LOO	56%	14%	7%	18%	0%	0%	2%	2%	1%
4LHO	48%	14%	7%	18%	8%	0%	2%	2%	1%
4HOO	56%	7%	14%	18%	0%	0%	2%	2%	1%
4HHO	48%	7%	14%	18%	8%	0%	2%	2%	1%
1LOH	32%	34%	17%	2%	0%	10%	2%	2%	1%
1LHH	26%	34%	17%	2%	6%	10%	2%	2%	1%
1HOH	32%	17%	34%	2%	0%	10%	2%	2%	1%
1HHH	26%	17%	34%	2%	6%	10%	2%	2%	1%
2LOH	53%	20%	10%	2%	0%	10%	2%	2%	1%
2LHH	44%	20%	10%	2%	9%	10%	2%	2%	1%
2HOH	53%	10%	20%	2%	0%	10%	2%	2%	1%
2HHH	44%	10%	20%	2%	9%	10%	2%	2%	1%
3LOH	25%	28%	14%	18%	0%	10%	2%	2%	1%
3LHH	20%	28%	14%	18%	5%	10%	2%	2%	1%
3HOH	25%	14%	28%	18%	0%	10%	2%	2%	1%
3HHH	20%	14%	28%	18%	5%	10%	2%	2%	1%
4LOH	46%	14%	7%	18%	0%	10%	2%	2%	1%
4LHH	38%	14%	7%	18%	8%	10%	2%	2%	1%
4HOH	46%	7%	14%	18%	0%	10%	2%	2%	1%
4HHH	38%	7%	14%	18%	8%	10%	2%	2%	1%
MID1	41%	18%	18%	10%	4%	5%	2%	2%	1%
MID2	41%	18%	18%	10%	4%	5%	2%	2%	1%
MID3	41%	18%	18%	10%	4%	5%	2%	2%	1%

Table A-III. Corning Environmental Laboratories - QCA Weight Percentages versus Target Oxide Weight Percentages

MID1	CELS wt%	TGT wt%	Diff
Al_2O_3	6.77	6.72	0.05
B_2O_3	2.83	3.21	-0.38
BaO	3.98	4.04	-0.06
CaO	12.80	13.30	-0.50
Fe_2O_3	20.10	21.05	-0.95
Na_2O	14.80	14.70	0.10
NiO	1.90	1.97	-0.07
PbO	2.77	2.94	-0.17
SiO_2	31.40	32.07	-0.67
Sum	97.35	100.00	

2HHH	CELS wt%	TGT wt%	Diff
Al_2O_3	14.80	14.38	0.42
B_2O_3	8.30	8.84	-0.54
BaO	4.30	4.33	-0.03
CaO	7.77	7.91	-0.14
Fe_2O_3	4.74	4.51	0.23
Na_2O	17.60	17.49	0.11
NiO	2.07	2.10	-0.03
PbO	2.97	3.15	-0.18
SiO_2	36.50	37.29	-0.79
Sum	99.05	100.00	

2MMM	CELS wt%	TGT wt%	Diff
Al_2O_3	7.71	7.30	0.41
B_2O_3	4.31	4.60	-0.29
BaO	4.48	4.50	-0.02
CaO	12.10	12.30	-0.20
Fe_2O_3	4.85	4.70	0.15
Na_2O	13.70	13.70	0.00
NiO	2.19	2.20	-0.01
PbO	3.17	3.30	-0.13
SiO_2	46.80	47.40	-0.60
Sum	99.31	100.00	

MMHO	CELS wt%	TGT wt%	Diff
Al_2O_3	1.18	0.00	1.18
B_2O_3	6.32	6.70	-0.38
BaO	4.19	4.20	-0.01
CaO	13.80	14.00	-0.20
Fe_2O_3	19.90	19.90	0.00
Na_2O	15.30	15.50	-0.20
NiO	2.00	2.00	0.00
PbO	2.93	3.00	-0.07
SiO_2	34.20	34.70	-0.50
Sum	99.82	100.00	

1,2MMH	CELS wt%	TGT wt%	Diff
Al_2O_3	14.50	14.60	-0.10
B_2O_3	3.54	3.70	-0.16
BaO	4.29	4.40	-0.11
CaO	15.50	16.20	-0.70
Fe_2O_3	4.80	4.60	0.20
Na_2O	17.90	17.90	0.00
NiO	2.07	2.10	-0.03
PbO	2.89	3.20	-0.31
SiO_2	32.50	33.30	-0.80
Sum	97.99	100.00	

3MMM	CELS wt%	TGT wt%	Diff
Al_2O_3	8.11	5.90	2.21
B_2O_3	2.02	2.10	-0.08
BaO	3.41	3.70	-0.29
CaO	12.70	14.10	-1.40
Fe_2O_3	32.00	34.40	-2.40
Na_2O	15.10	15.50	-0.40
NiO	1.65	1.80	-0.15
PbO	2.37	2.70	-0.33
SiO_2	20.90	19.80	1.10
Sum	98.26	100.00	

Table A-IV. 2MMM Standard Used with Fundamental Parameters to Predict the Compositional Space (in wt%)

Glasses	Na_2O	Al_2O_3	BaO	CaO	Fe_2O_3	NiO	PbO	SiO_2	B_2O_3
1,2MMHa	17.85	14.64	4.33	15.70	4.86	2.11	2.94	32.76	4.12
1,2MMHa1	17.86	14.59	4.31	15.65	4.84	2.10	2.95	32.64	4.36
1LOO	15.88	1.12	4.41	27.34	4.77	2.18	2.86	37.94	2.82
1LHO	15.79	1.60	4.45	26.96	4.75	2.18	3.10	32.24	8.24
1HOO	30.17	1.71	4.44	13.63	4.75	2.19	3.05	37.43	1.95
1HHO	30.78	1.21	4.57	13.77	4.83	2.20	3.17	31.78	7.01
1LOHc	14.78	14.41	4.06	24.74	4.61	2.00	2.59	26.48	5.63
1LHH	15.10	14.83	4.15	25.31	4.62	2.04	2.70	22.03	8.53
1HHHd	27.67	13.90	3.98	13.01	4.87	1.97	2.10	21.37	10.44
2MMM	13.71	7.75	4.50	12.15	4.89	2.20	3.19	47.08	3.84
2LOO	9.49	0.46	4.62	16.61	4.95	2.27	3.28	57.06	0.57
2LHO	9.29	1.04	4.59	16.46	4.93	2.25	3.27	48.49	8.99
2HOO	18.77	0.37	4.58	8.41	5.01	2.30	3.30	56.92	0.00
2HHO	18.50	0.59	4.73	8.42	4.97	2.28	3.33	48.67	7.81
2LOH	9.12	14.57	4.29	15.37	4.96	2.10	3.03	44.39	1.49
2LHH	8.89	14.72	4.30	15.37	4.70	2.08	3.05	36.85	9.37
2HOH	17.78	14.62	4.35	7.86	4.72	2.13	3.09	44.46	0.31
2HHH	17.55	14.78	4.37	7.83	4.83	2.11	3.04	36.75	8.06
3MMM	14.77	7.95	3.40	12.53	30.29	1.56	2.27	20.63	5.91
3LOO	10.72	1.57	3.60	17.97	32.56	1.66	2.41	25.29	3.53
3LHO	10.68	2.40	3.60	17.74	31.74	1.54	2.41	21.57	7.64
3HOO	20.53	1.14	3.35	8.68	30.80	1.52	2.31	25.71	5.27
3HHO	19.85	1.70	3.55	8.83	31.30	1.60	2.36	23.16	6.97
3LOHc	8.97	17.12	3.01	14.94	26.58	1.13	2.06	24.36	1.14
3LHH	9.06	18.15	3.10	15.21	27.36	1.37	2.05	16.22	6.80
3HHH	20.77	11.72	3.45	8.74	30.90	1.51	2.23	14.10	5.90
4MMM	8.96	7.03	3.81	7.82	25.94	1.35	2.65	35.95	5.79
4LOO	5.34	0.54	3.61	9.28	31.68	1.37	2.56	40.16	4.78
4HHO	10.31	0.62	3.68	4.60	31.60	1.63	2.54	33.91	10.43
6LOH	6.98	13.88	4.01	11.85	18.89	1.26	2.61	38.41	1.42
6LHH	6.51	13.94	3.87	11.13	20.71	1.15	2.71	30.99	8.30
6HHH	12.68	13.90	3.90	5.51	22.13	1.10	2.68	30.00	7.40
MID1	14.57	6.77	4.03	12.95	19.91	1.90	2.78	31.67	4.74
MID2	14.74	6.88	4.03	12.85	20.53	1.87	2.78	31.43	4.21
MID3	14.56	7.23	3.98	12.82	20.36	1.88	2.75	31.43	4.31
MMOO	15.27	1.01	4.08	13.45	19.26	1.95	2.87	40.24	1.19
MMHO	15.18	1.17	4.17	13.67	19.17	1.94	2.87	33.87	7.27

Table A-IV. (Continued)

Glasses	Na_2O	Al_2O_3	BaO	CaO	Fe_2O_3	NiO	PbO	SiO_2	B_2O_3
4HOOA-a	10.91	0.29	3.84	4.85	30.09	1.70	2.62	40.77	4.25
4MMMa1	8.92	7.01	3.82	7.85	26.02	1.36	2.66	35.95	5.71
2LOHZ	8.91	14.73	4.30	15.46	4.69	2.10	3.04	44.73	1.36
2LOHZA1	9.00	14.71	4.31	15.48	4.71	2.11	3.08	44.76	1.16
2HHOZ	18.59	0.60	4.74	8.42	5.00	2.29	3.34	48.58	7.75
2MMMa1	13.65	7.73	4.50	12.13	4.87	2.20	3.19	46.83	4.21

Table A-V. 3MMM Standard Used with Fundamental Parameters to Predict the Compositional Space (in wt%)

Glasses	Na_2O	Al_2O_3	BaO	CaO	Fe_2O_3	NiO	PbO	SiO_2	B_2O_3
1,2MMHa	17.89	14.69	4.29	15.65	5.09	2.17	2.97	32.75	4.52
1,2MMHa1	17.95	14.68	4.31	15.70	5.11	2.18	3.01	32.96	4.09
1LOO	15.89	1.12	4.39	27.18	4.98	2.23	2.88	38.06	3.27
1LHO	15.86	1.61	4.42	26.84	4.97	2.25	3.14	32.43	8.47
1HOO	29.81	1.68	4.38	13.51	4.93	2.25	3.08	37.10	3.27
1HHO	30.44	1.22	4.50	13.65	5.03	2.26	3.21	31.61	8.07
1LOHc	14.85	14.57	4.03	24.58	4.80	2.06	2.60	26.53	5.98
1LHH	15.14	14.87	4.09	25.05	4.79	2.09	2.71	22.02	9.24
1HHHd	29.88	12.83	3.81	12.47	4.91	1.96	2.07	19.84	12.23
2MMM	13.87	7.68	4.45	12.08	5.08	2.26	3.23	46.52	4.83
2LOO	9.67	0.46	4.57	16.52	5.17	2.33	3.33	56.84	1.12
2LHO	9.48	1.03	4.57	16.34	5.13	2.31	3.31	48.17	9.66
2HOO	18.85	0.36	4.49	8.34	5.20	2.36	3.32	56.54	0.55
2HHO	18.66	0.59	4.71	8.45	5.24	2.37	3.40	48.72	7.87
2LOH	9.34	14.49	4.27	15.33	5.20	2.17	3.07	44.40	1.74
2LHH	9.04	14.67	4.26	15.31	4.91	2.15	3.09	36.74	9.84
2HOH	17.97	14.61	4.35	7.88	4.97	2.21	3.16	44.62	0.24
2HHH	17.68	14.76	4.36	7.84	5.04	2.18	3.08	36.74	8.34
3MMM	15.14	8.14	3.42	12.80	32.26	1.67	2.40	21.18	2.99
3LOO	11.00	1.59	3.60	17.15	34.29	1.77	2.50	25.69	1.41
3LHO	10.92	2.43	3.58	17.93	33.56	1.63	2.51	21.84	5.61
3HOO	20.72	1.15	3.34	8.78	32.48	1.61	2.41	25.82	3.71
3HHO	20.39	1.72	3.57	9.02	33.38	1.71	2.48	25.82	3.71
3LOHc	9.14	17.25	2.98	14.98	27.80	1.19	2.12	24.55	0.00
3LHH	9.34	18.50	3.12	15.45	29.09	1.46	2.15	16.57	4.34
3HHH	21.65	11.95	3.48	8.95	33.11	1.63	2.36	14.34	2.52
4MMM	9.09	7.09	3.86	7.98	27.56	1.44	2.78	36.63	3.57
4LOO	5.55	0.55	3.68	9.53	34.09	1.49	2.73	41.21	1.17
4HHO	10.57	0.62	3.69	4.68	33.55	1.73	2.66	34.39	8.11
6LOH	7.07	14.04	4.03	11.96	19.88	1.32	2.69	38.87	0.15
6LHH	6.59	14.03	3.85	11.21	21.64	1.20	2.77	31.40	7.30
6HHH	12.80	14.01	3.90	5.56	23.32	1.16	2.78	30.27	6.20
MID1	14.73	6.88	4.03	13.05	20.90	1.99	2.85	31.97	3.60
MID2	14.89	6.96	4.06	12.98	21.59	1.97	2.86	31.90	2.80
MID3	14.66	7.29	3.97	12.89	21.30	1.97	2.82	31.67	3.43
MMOO	15.44	0.99	4.10	13.55	20.14	2.03	2.93	40.65	0.18
MMHO	15.37	1.18	4.18	13.78	20.15	2.04	2.96	34.07	6.28
4HOOA-a	11.14	0.29	3.88	4.94	32.00	1.81	2.75	41.45	1.74
4MMMa1	9.08	7.06	3.84	7.94	27.46	1.44	2.77	36.33	4.08

Table A-V. (Continued)

Glasses	Na_2O	Al_2O_3	BaO	CaO	Fe_2O_3	NiO	PbO	SiO_2	B_2O_3
2LOHZ	9.07	14.70	4.26	15.39	4.91	2.17	3.06	44.46	2.00
2LOHZa1	9.12	14.71	4.27	15.41	4.92	2.17	3.12	44.57	1.71
2HHOZ	18.96	0.61	4.69	8.38	5.21	2.35	3.38	48.17	8.52
2MMMa1	13.91	7.67	4.44	12.10	5.09	2.27	3.23	46.78	4.52

Table A-VI. Plot of Na_2O CELs Wt % vs FP Wt %. The 3MMM standard was used. The line is the perfect correlation line

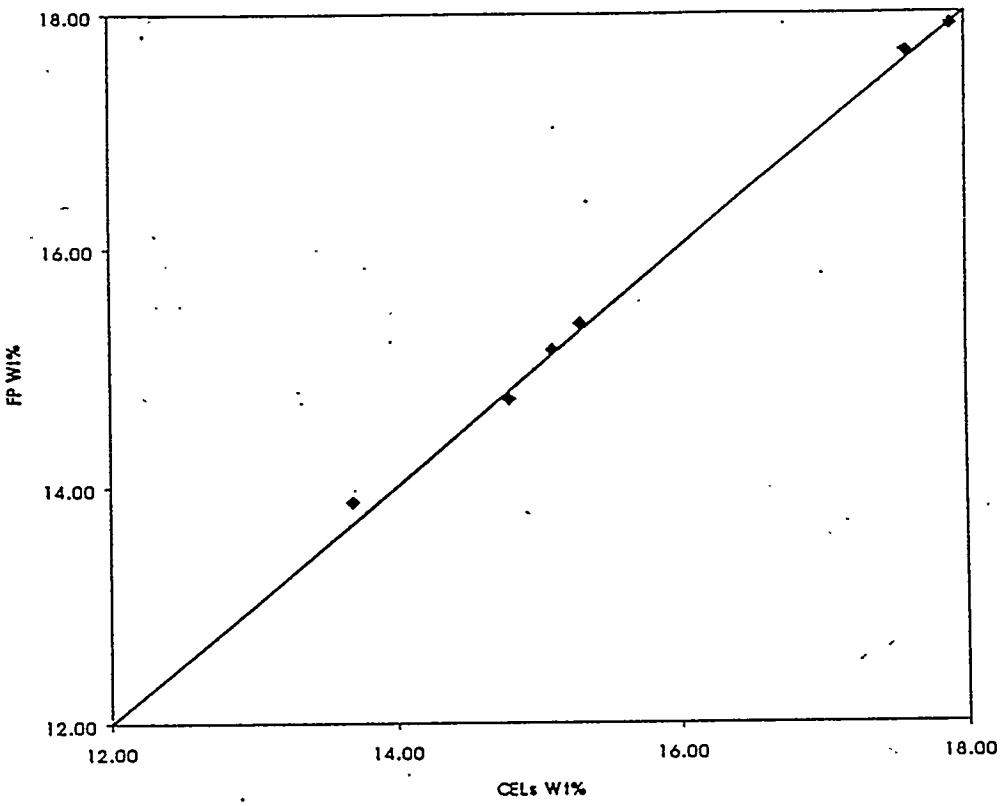

Table A-VII. Plot of Al_2O_3 CELs Wt % vs FP Wt %. The 3MMM standard was used. The line is the perfect correlation line.

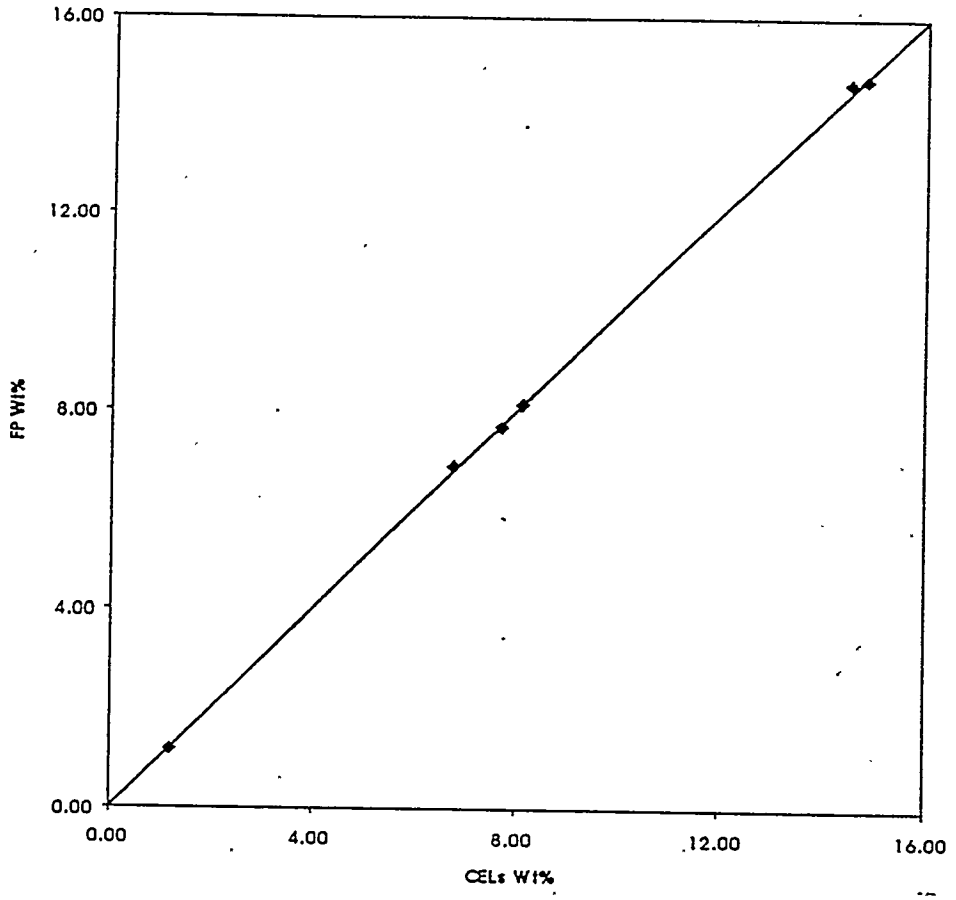

Table A-VIII. Plot of BaO CELs Wt % vs FP Wt %. The 3MMM standard was used. The line is the perfect correlation line.

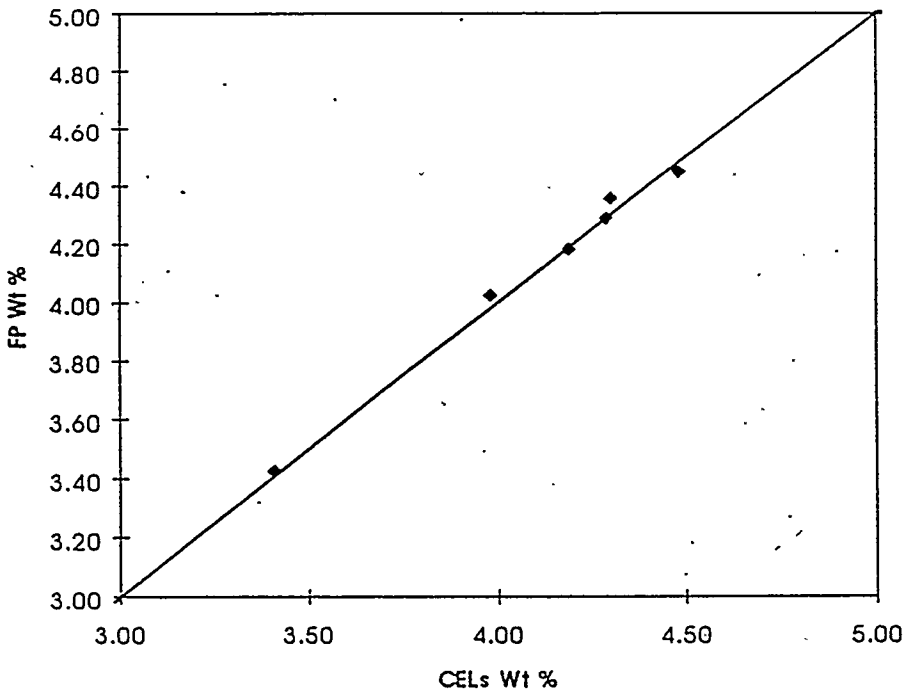

Table A-IX. Plot of CaO CELs Wt % vs FP Wt %. The 3MMM standard was used. The line is perfect correlation line.

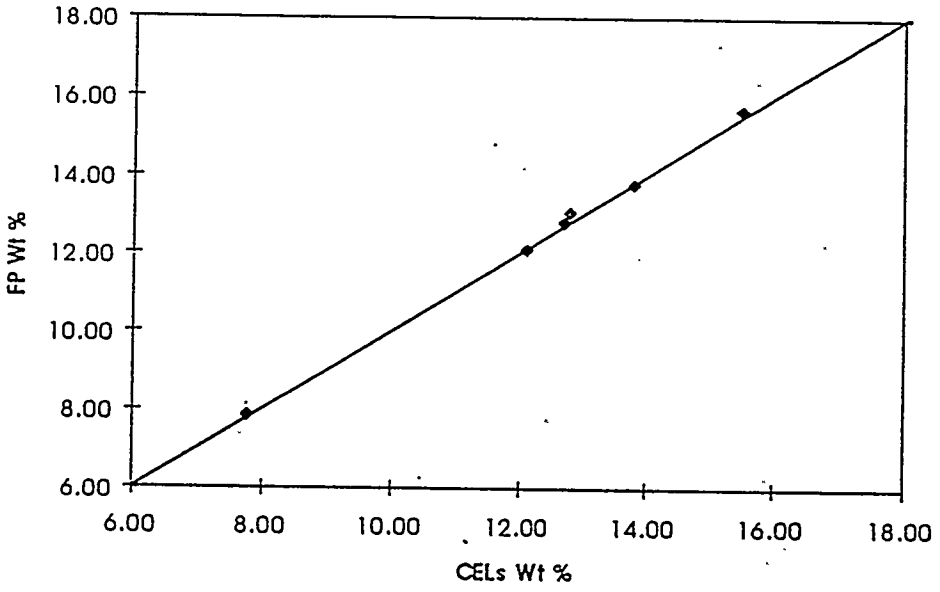

Table A-X. Plot of Fe2O3 CELs Wt % vs FP Wt %. The 3MMM standard was used. The line is the perfect correlation line.

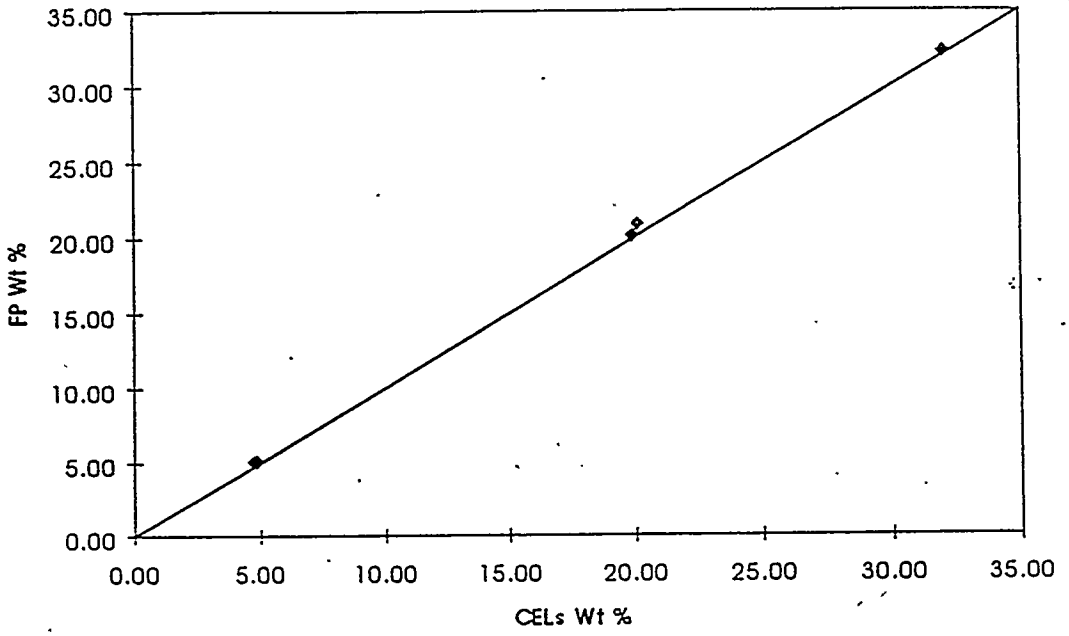

Table A-XI. Plot of NiO CELs Wt % vs FP Wt %. The 3MMM standard was used. The line is the perfect correlation line.

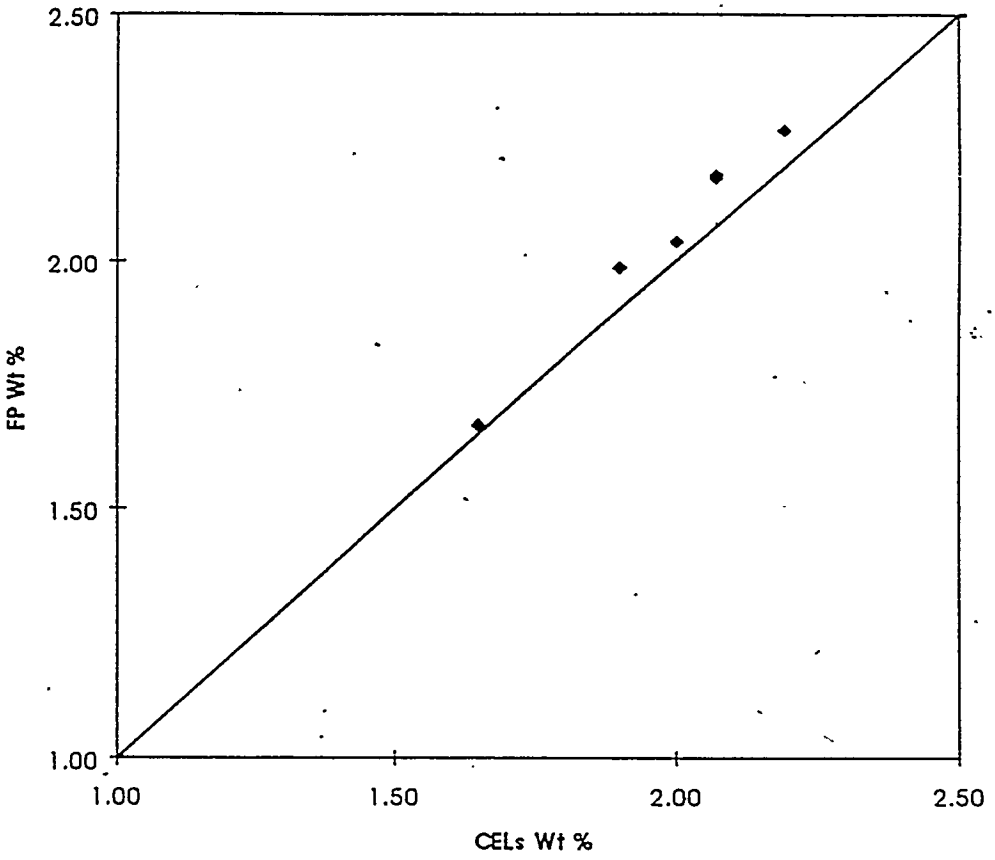

Table A-XII. Plot of PbO CELs Wt % vs FP Wt %. The 3MMM standard was used. The line is the perfect correlation line.

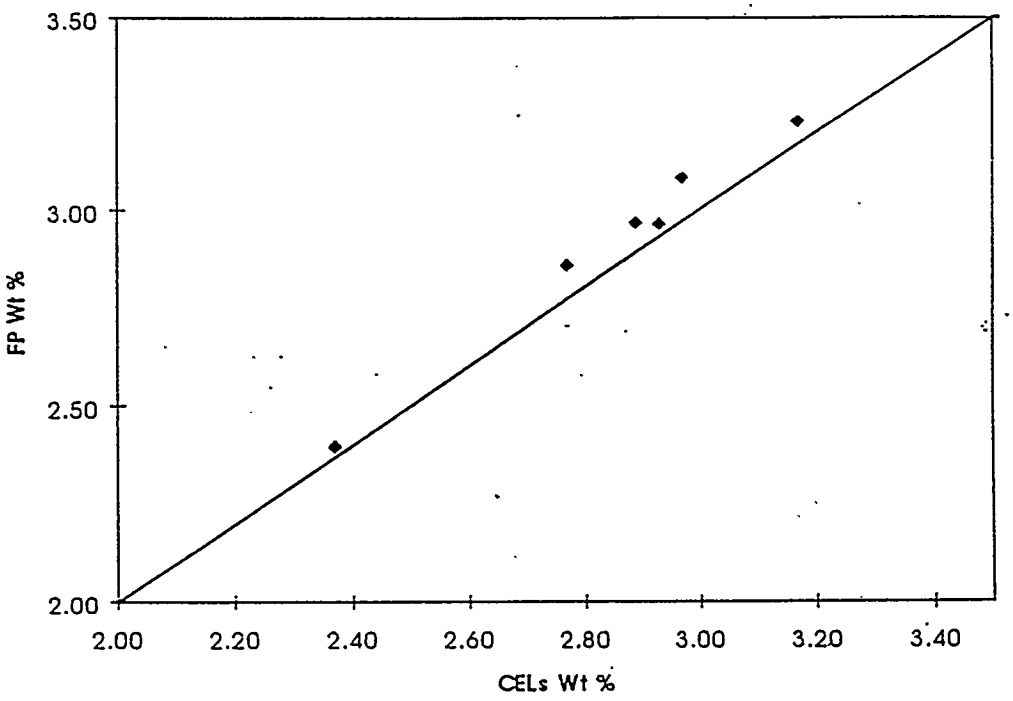

Table A-XIII. Plot of SiO_2 CELs Wt % vs FP Wt %. The 3MMM standard was used. The line is the perfect correlation line.

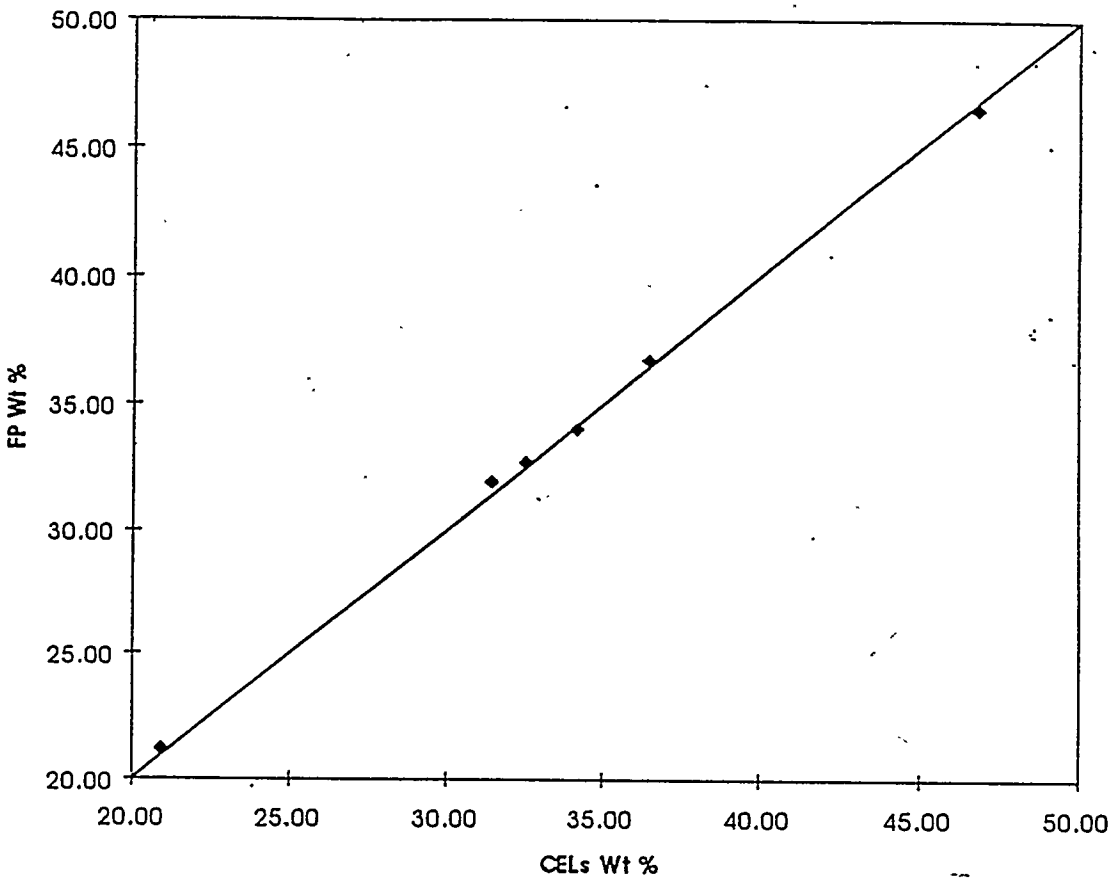

Table A-XIV. Plot of B_2O_3 CELs Wt % vs FP Wt %. The 3MMM standard was used. The line is the perfect correlation line.

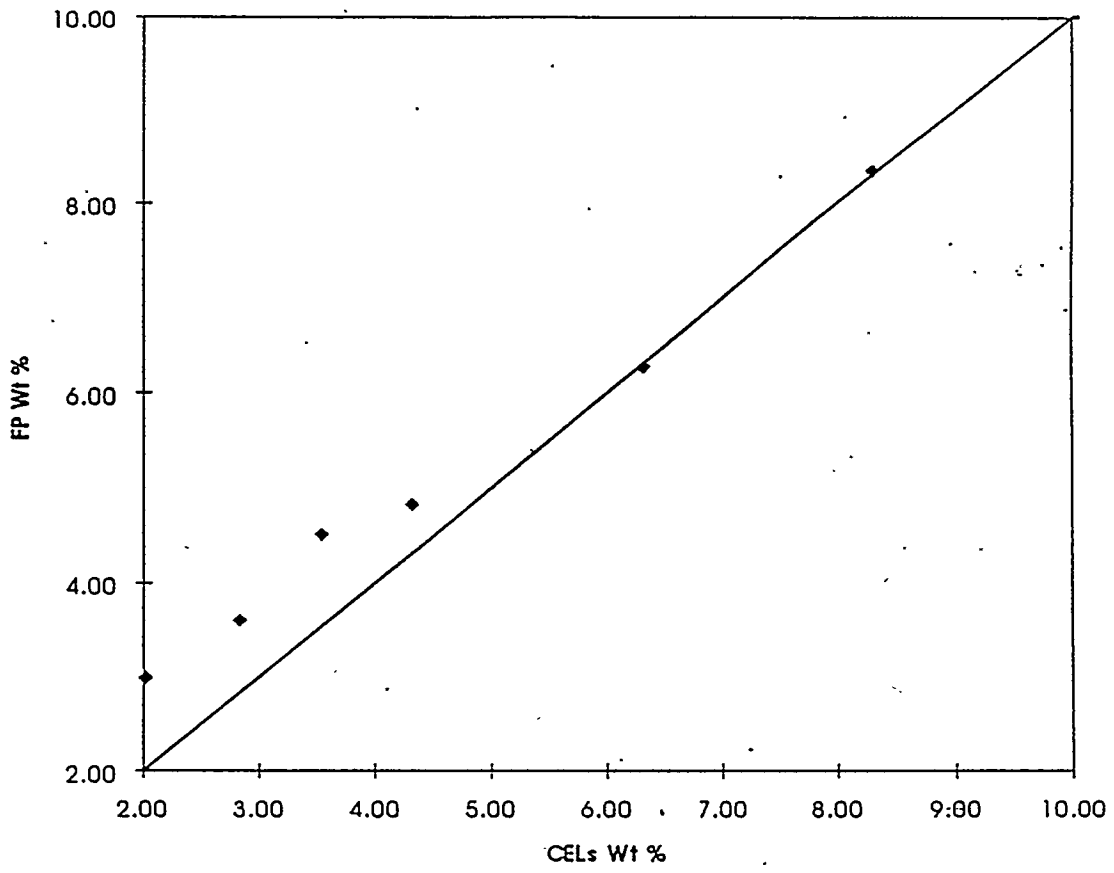

Appendix B

Toxicity Characteristic Leaching Procedure Test

The leaching characteristics of the compositional space glasses were analyzed by TCLP and PCT on an extended basis to include glass forming materials.

TCLP was conducted on the constant surface area pellets developed especially for this research to meet the requirements of the fourth and fifth experimental objectives. Each pellet had a surface area of approximately 11 cm^2. The density of the glasses ranged from 2.75 to 3.40 g/cm^3. This corresponds to 0.306 cm^2 of glass/cm^3 of leachate in the TCLP test. This constant surface area is a new concept in TCLP analysis and can be used to gain greater consistency in the TCLP results. The results of the TCLP tests appear in Table B-I. The values are in mg/L.

In order to evaluate the results from the TCLPs for the glasses for the leaching concentrations, it is first necessary to know the limits for comparison purposes. The RCRA toxicity characteristics and LDR limits appear in Table B-II.

By comparing the results of Table B-I with the limits from Table B-II, several observations are apparent. Barium fails TCLP for only one glass, 3HOH. Lead exceeds the RCRA standards for TCLP for glasses 1LOO, 1LHO. 1HOO, 1LHH, 1HOH, 2HHO, 3HOH, and 3HHH. The RCRA limits on nickel are exceeded for all of the 1-Space glasses as well as 2LHO, 2HHO, 2LHH, 2HHH, MIDs 1, 2, and 3, MMOO, and MMHO. The main conclusion to be drawn from these data is that the 1-Space glasses are the least durable for lead and nickel. Additionally, there seems to be increased leaching and some correlation between boron addition and any levels of Na for some of the glasses. Also, addition of Al does not necessarily promote durability for some of the glasses with levels of Na and boron. Plots of these results for 1- Space through 4-Space appear in Tables B-III through B-X.

Table B-I. TCLP Leaching Data From the Compositional Space. All values are in mg/L.

Glass	Fe	Al	Pb	Ba	B	Si	Ni	Ca
1LOO	0.61	0.10	14.42	50.18	0.04	39.31	17.69	260.99
1LHO	1.08	0.10	11.58	64.50	29.47	55.67	26.86	343.20
1HOO	0.46	0.10	10.56	64.89	0.13	32.44	24.49	169.43
1HHO	0.43	0.10	2.53	75.63	35.80	56.33	27.99	195.97
1LOH	0.53	6.95	3.10	10.12	0.04	16.33	2.04	47.17
1LHH	4.29	26.93	11.8	34.94	15.56	46.45	7.75	174.75
1HOH	0.46	7.33	8.29	65.62	0.04	20.65	6.07	88.52
2LOO	0.03	0.10	0.20	0.73	0.04	2.58	0.05	1.30
2LHO	0.27	0.10	1.24	3.01	1.51	3.62	0.95	7.29
2HOO	0.03	0.10	0.20	1.22	0.04	3.05	0.22	0.98
2HHO	1.51	0.10	17.45	37.67	23.19	25.02	15.89	52.77
2LOH	0.09	0.10	0.20	0.84	0.04	3.49	0.15	1.13
2LHH	0.17	0.25	0.34	1.32	0.49	4.65	0.34	2.32
2HOH	0.06	0.10	0.20	0.90	0.04	3.55	0.11	0.58
2HHH	0.27	0.96	0.98	2.06	0.94	6.26	0.60	2.18
3LOO	0.18	0.10	0.24	1.79	0.04	4.13	0.05	9.25
3LHO	0.09	0.10	0.30	2.13	0.50	4.82	0.05	7.02
3HOO	0.73	0.10	0.35	2.65	0.04	4.58	0.05	6.70
3HHO	1.08	0.10	1.25	5.40	1.42	7.57	0.14	8.84
3LOH	0.79	8.68	1.74	3.89	0.04	15.69	0.05	12.85
3LHH	0.24	5.27	0.87	2.53	0.61	8.10	0.05	7.57
3HOH	0.09	0.10	25.81	109.94	0.04	24.14	0.24	223.60
3HHH	0.19	3.57	12.71	56.69	21.24	17.78	0.05	120.01
4LOO	0.22	0.10	0.20	0.60	0.04	2.99	0.05	0.35
4LHO	0.36	0.10	0.20	0.78	0.04	3.23	0.06	0.55
4HOO	0.28	0.10	0.20	0.58	0.04	2.94	0.09	0.18
MID1	1.52	0.76	1.05	2.47	0.55	5.82	0.60	4.47
MID2	1.16	0.75	0.95	1.77	0.39	5.32	0.44	3.78
MID3	0.69	0.37	0.98	2.48	0.37	6.76	0.71	4.96
MMOO	0.63	0.10	0.51	1.64	0.04	4.04	0.39	3.01
MMHO	1.21	0.10	1.50	4.27	1.65	6.76	1.16	8.61
4HOOA	0.90	0.10	0.20	0.86	0.04	3.25	0.11	0.48
4HOOE	1.07	0.10	0.20	1.04	0.56	3.80	0.07	0.64
4LOOE	0.47	0.10	0.20	0.75	0.15	3.28	0.08	0.73
4LHOE	0.62	0.10	0.20	1.04	0.29	3.72	0.06	1.01

Note - The detection limit (in mg/L) for Al is 0.10; for Pb is 0.20; for B is 0.04; for Ni is 0.05.

Table B-II. TCLP and RCRA LDR Regulatory Limits

Waste Codes	Regulated Metal	RCRA TCLP* Limit (mg/L)	RCRA LDR** Limit (mg/L)
		Characteristic Waste Codes	
D005	Barium	100.0	100.0
D008	Lead	5.0	5.0
		Listed Waste Codes	
F006***	Nickel	N/A	0.32

* TCLP: Maximum concentration of contaminants (40 CFR 261.24; see 55 FR 11862, March 12, 1990) as determined by Toxic Characteristic Leaching Procedure (40 CFR 261, Appendix I)

** LDR: concentration based standards for Land Disposal Requirements, (40 CFR 268.41 and 268.43; see 55 FR 22689, June 1, 1990)

*** F006: Hazardous Waste from Non-Specific Sources; Wastewater treatment sludges from electroplating operations.

Table B-III. Plot of TCLP Results for 1-Space for Fe, Al, Pb, Ba

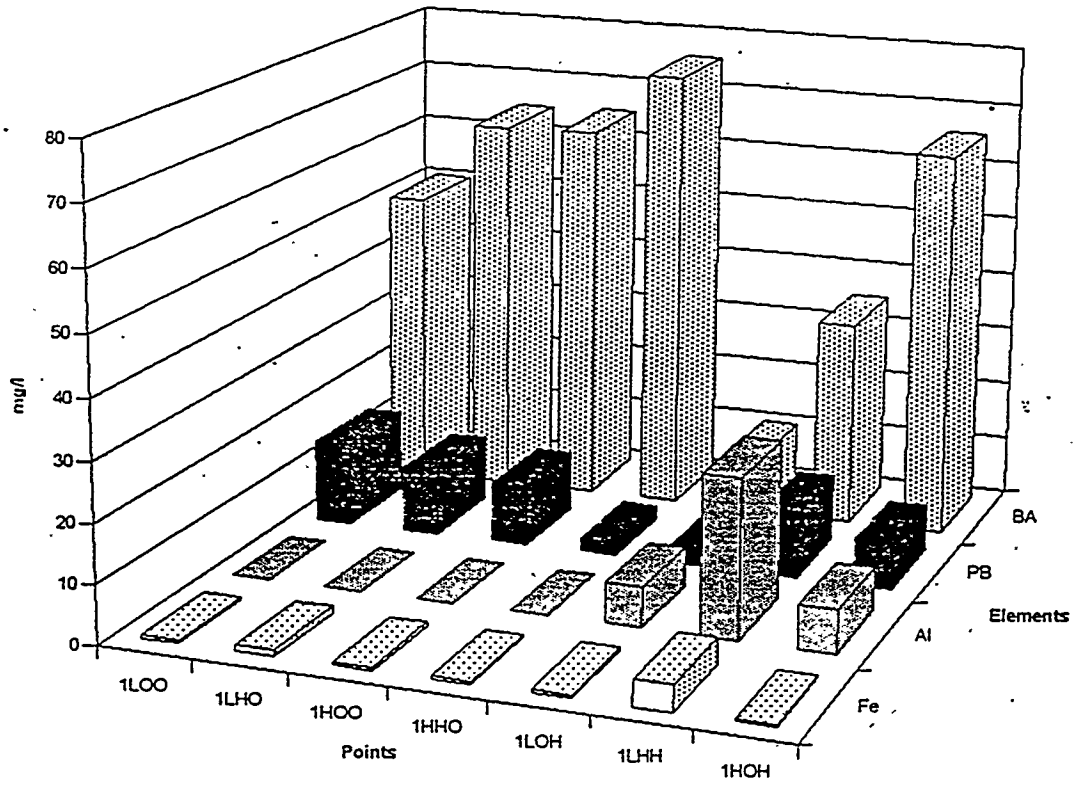

Table B-IV. Plot of TCLP Results for 1-Space for B, Si, Ni, Ca

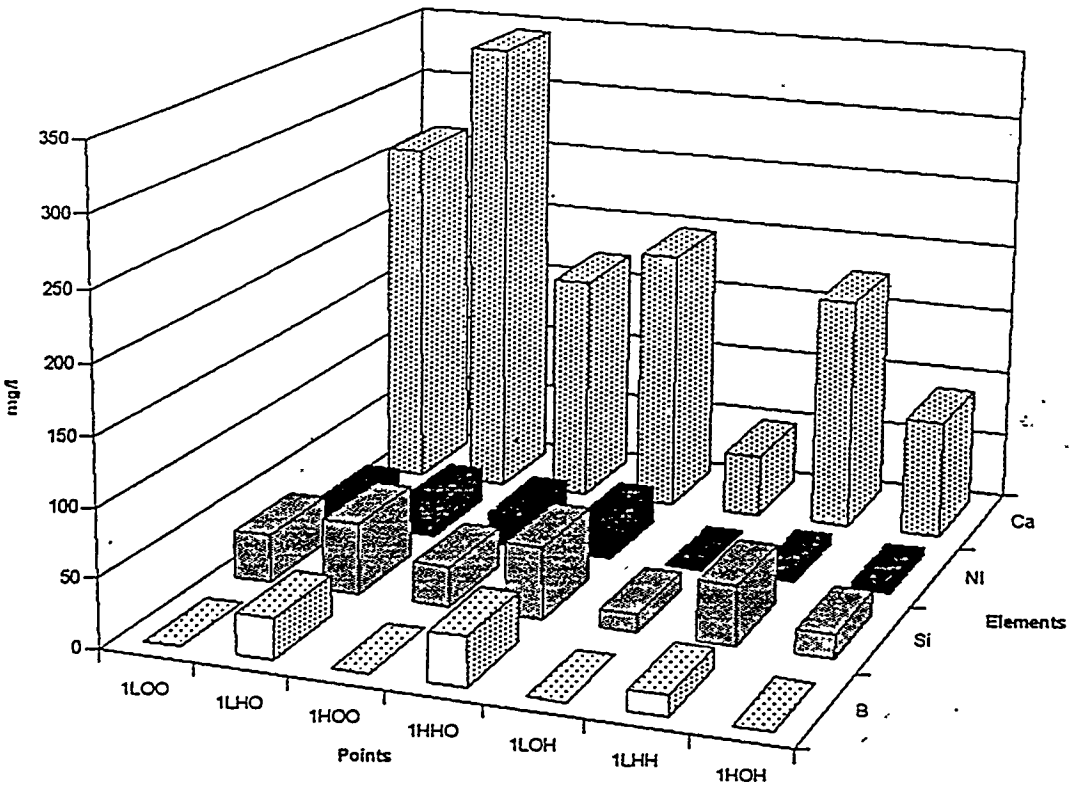

Table B-V. Plot of TCLP Results for 2-Space for Fe, Al, Pb, Ba

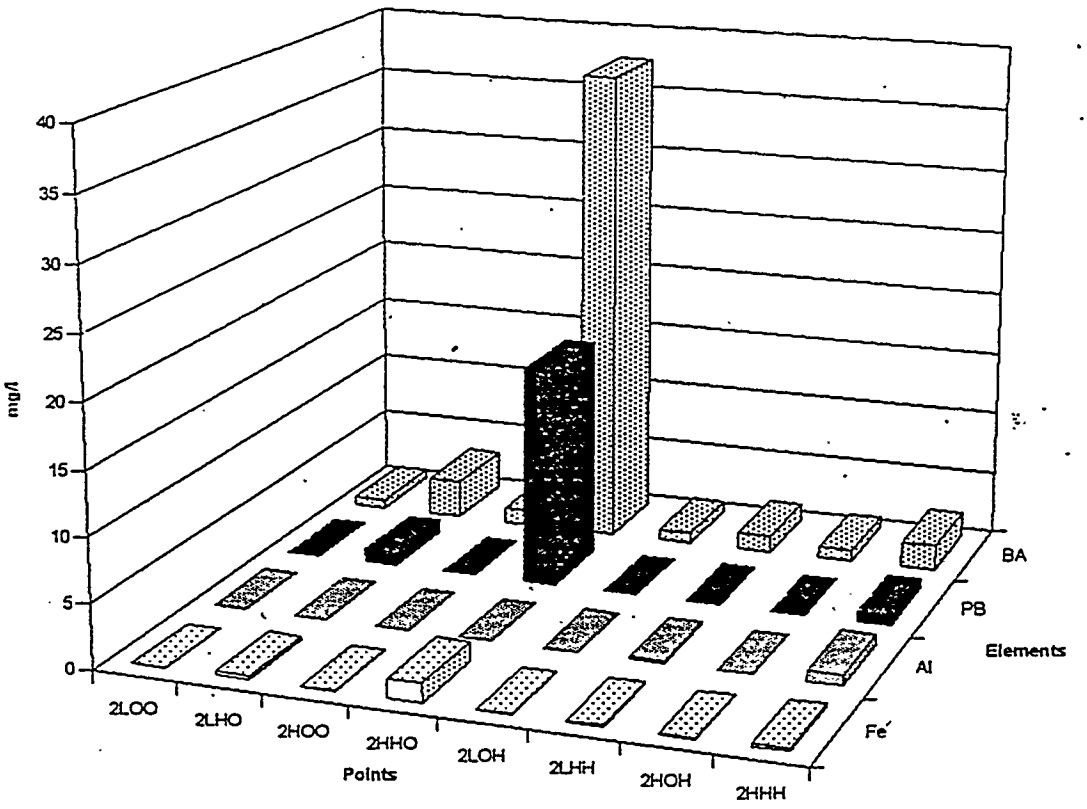

Table B-VI. Plot of TCLP Results for 2-Space for B, Si, Ni, Ca

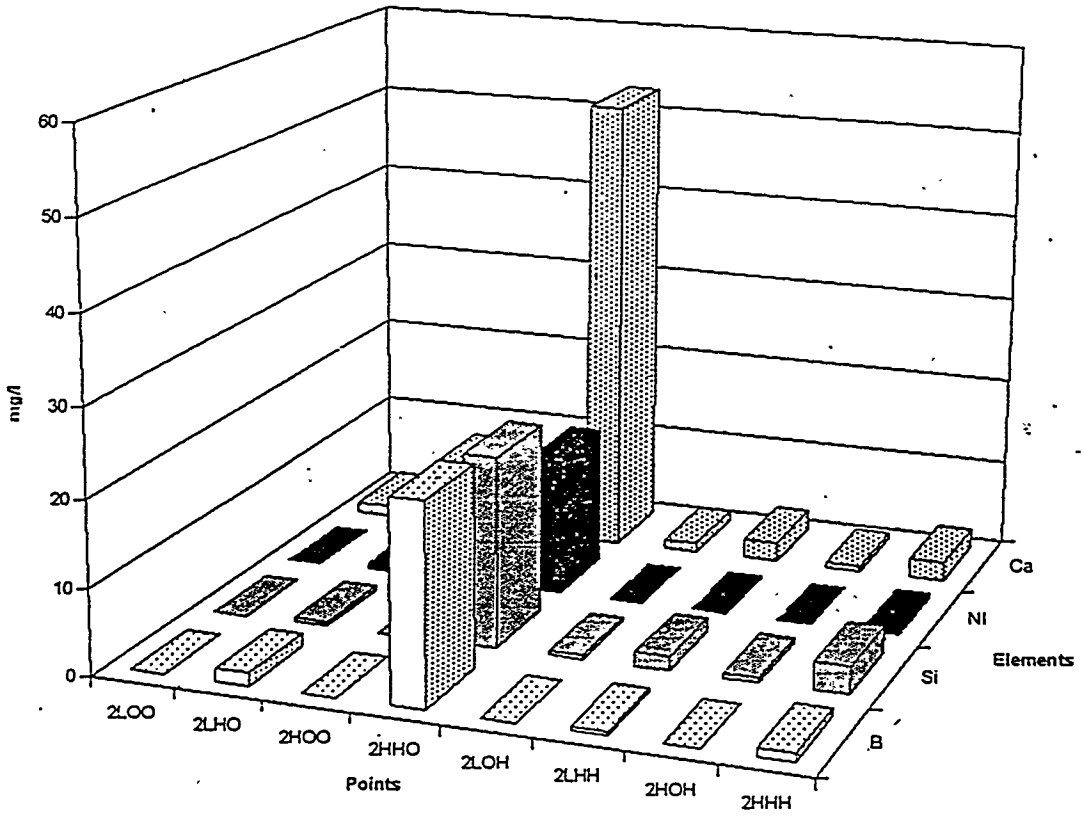

Table B-VII. Plot of TCLP Results for 3-Space for Fe, Al, Pb, Ba

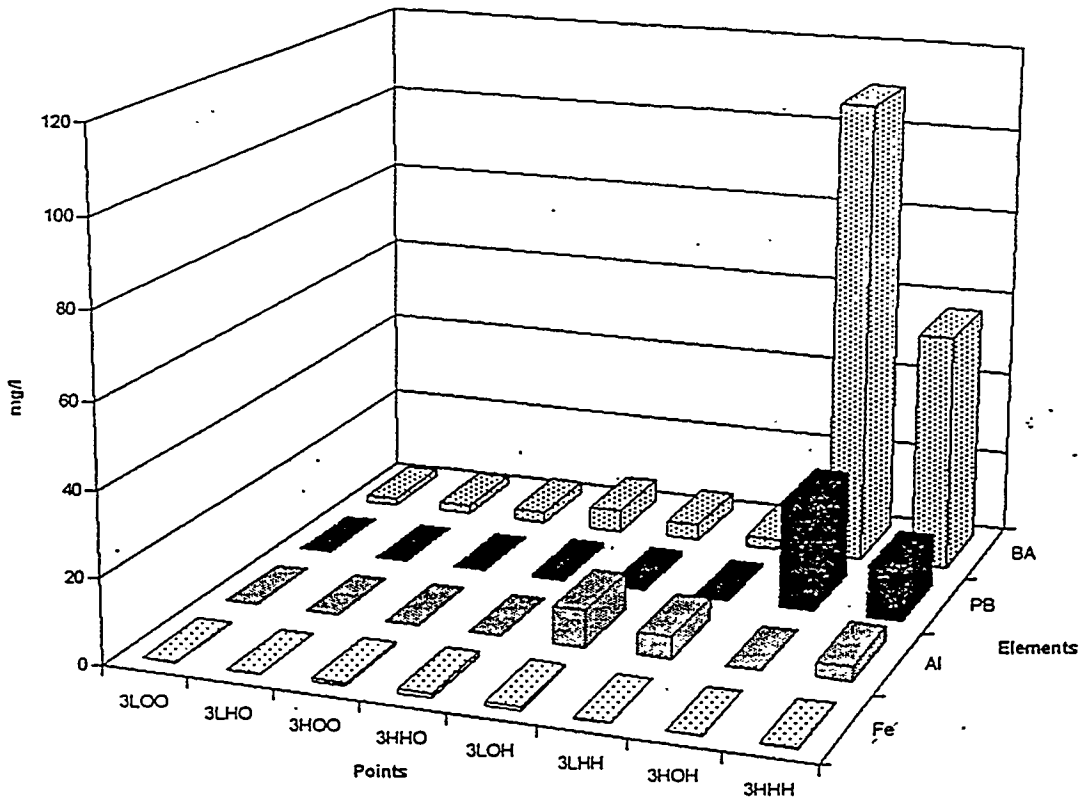

Table B-VIII. Plot of TCLP Results for 3-Space for B, Si, Ni, Ca

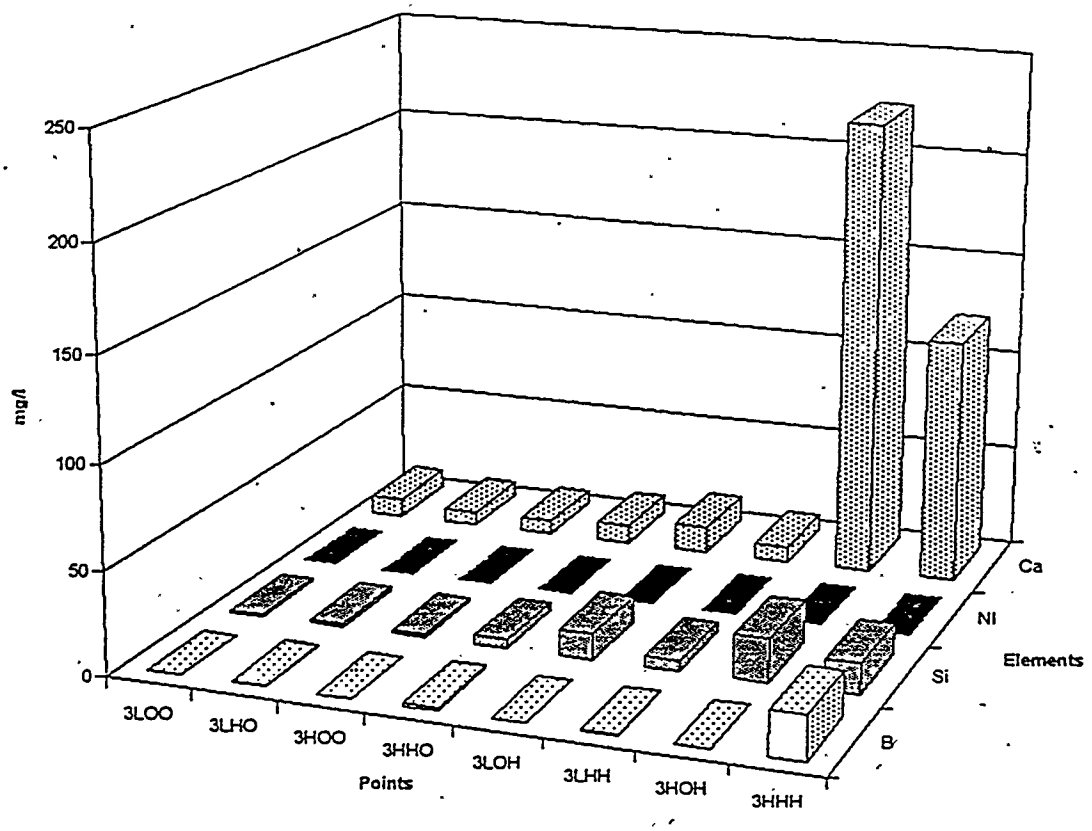

Table B-IX. Plot of TCLP Results for 4-Space and Midpoints for Fe, Al, Pb, Ba

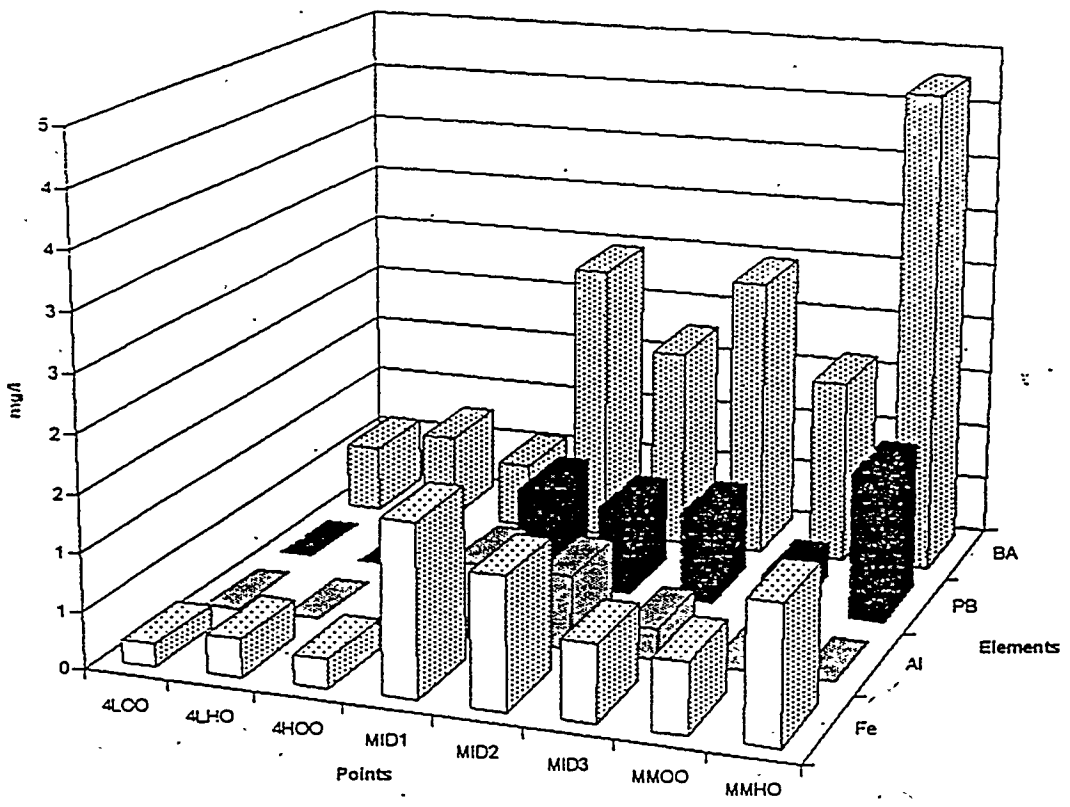

Table B-X. Plot of TCLP Results for 4-Space and Midpoints for B, Si, Ni, Ca

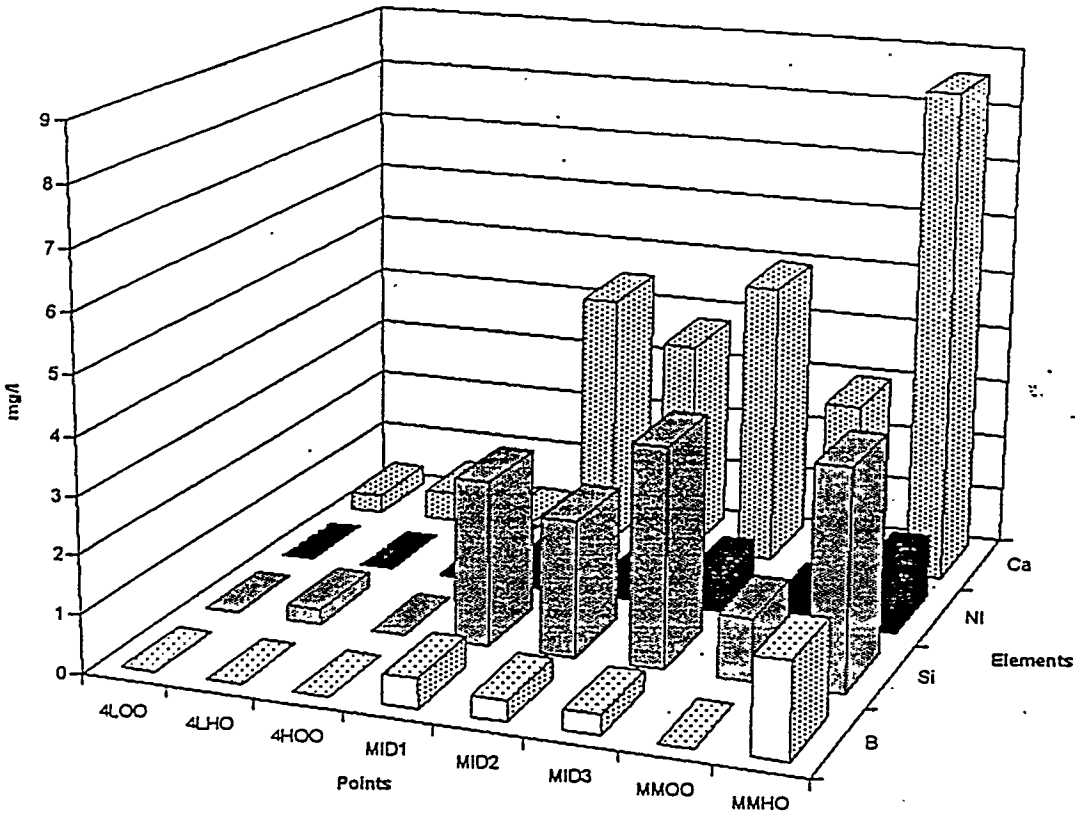

Appendix C

Product Consistency Test

The second test of the leaching characteristics of the glasses was performed with the PCT (Jantzen *et al.*, 1987). The PCT was conducted on an extended basis to include glass forming materials on the constant surface area forms after appropriate milling to a size appropriate for this test. The PCT leachate concentrations, in mg/L corrected for blanks, for B, Si, Na, Al, and Pb along with the initial and final pH values appear in Table C-I. The $\log_{10}$ normalized release for all nine elements are presented in Table C-II. The blanks in the table indicate that that particular glass did not contain the associated element. One conclusion to be drawn from the data is that the 1-Space glasses are the least durable. Additionally, the data from Table C-I correlates to an extent with the results from the TCLP results in Table B-I. Both tests suggest that the same glasses lack durability. For example, both tests confirm that the 1-Space glasses are not durable. The major difference between the 4-Space and the 2-Space is the iron. And yet there is very little difference between the durabilities of these two glass spaces. High levels of iron do not appear to decrease the durability of the 4-Space. The major difference between the 3-Space and the 1-Space is also the iron. In this case higher iron content appears to improve durability.

Plots of selected leaching results for the four sub-spaces appear in Tables C-III through C-VI. These figures suggest that an increased leaching rate tends to follow increases in the Na content and/or the B content. Also, the addition of Al generally enhances the durability of the glasses. For example, in Table C-IV the 2-Space glasses with Al have lower leaching then the corresponding glasses without Al. This trend tends to follow for the 1-, 2-, and 4-Spaces, but not the 3-Space.

Table C-I. Product Consistency Test Data

Glass	pH init	pH final	Leachate concentration (ppm) corrected for blanks (Values are averages of 3 measurements)					
			B	Si	Na	Na*	Al	Pb
1LOO	6.93	12.87	0.79	71.82	1869.33	1599.54	2.99	8.84
1HOO	6.93	13.37	0.45	659.71	7787.01	6358.19	42.67	93.14
1LHO	6.93	12.59	105.28	16.98	1033.41	874.58	2.22	4.65
1HHO	6.93	13.57	1307.67	1485.84	15538.34	12742.18	11.46	45.38
1LOH	6.77	11.56	-0.02	17.10	124.85	109.58	18.12	0.16
1HOH	6.60	13.20	1.21	82.72	14217.24	12796.60	921.19	66.55
1LHH	6.60	11.66	8.83	9.87	156.81	133.53	24.29	0.37
1HHH	6.84	13.15	388.07	100.53	9267.31	7566.73	694.30	47.20
2LOO	6.93	11.10	0.22	60.45	43.32	37.89	-0.01	0.00
2HOO	6.60	12.23	0.25	115.92	559.60	480.88	0.15	1.27
2LHO	6.60	10.48	11.95	67.70	43.02	38.48	0.15	0.30
2HHO	6.77	11.60	30.96	166.37	318.73	282.12	0.27	0.30
2LOH	6.77	10.48	-0.04	16.28	13.51	11.70	4.71	0.01
2HOH	6.81	11.55	0.03	30.32	110.32	101.89	9.69	0.20
2LHH	6.60	10.18	3.25	13.54	13.39	11.51	5.19	0.30
2HHH	6.77	11.06	4.83	22.69	62.98	56.95	9.15	0.08
3LOO	6.60	11.32	0.17	17.15	38.70	34.33	0.19	0.30
3HOO	6.77	12.61	-0.03	111.39	1986.61	1612.23	4.14	1.82
3LHO	6.60	11.19	2.98	15.56	34.82	30.36	0.62	0.30
3HHO	6.60	10.23	16.06	68.39	781.54	649.88	6.90	0.30
3LOH	6.77	10.58	-0.09	10.69	17.72	15.63	9.56	0.00
3HOH	6.60	12.88	1.05	126.63	3494.81	2950.90	171.94	9.33
3LHH	6.77	11.24	3.84	6.63	35.43	32.51	20.75	0.00
3HHH	6.60	12.78	118.61	43.44	3221.93	2869.66	251.80	12.26
4LOO	6.81	10.25	0.17	33.63	18.68	17.39	0.63	0.01
4HOO	6.60	11.28	0.27	48.50	109.67	85.72	0.73	0.30
4LHO	6.60	9.96	3.42	25.31	17.54	14.83	0.15	0.30
4HHO	6.60	11.14	10.83	55.55	97.38	91.71	0.73	0.00
6LOH	6.60	10.60	-0.05	15.80	20.31	19.63	5.78	0.00
6HOH	6.60	11.07	-0.03	24.36	56.21	53.39	9.26	0.01
6LHH	6.60	10.12	2.65	12.36	12.68	12.02	5.87	0.00
6HHH	6.60	10.64	3.79	18.22	35.59	33.77	9.34	0.00
MID1	6.93	11.43	1.78	19.71	83.59	74.10	5.12	0.00
MID2	6.93	11.34	2.16	19.52	74.79	66.32	4.97	0.00
MID3	6.60	11.33	2.36	21.90	90.18	73.06	5.69	0.30
1,2MMH	6.84	11.51	2.46	23.55	101.03	82.37	11.49	0.20
2MMM	6.84	11.00	2.30	29.46	43.62	39.84	3.22	0.07
3MMM	6.84	11.71	2.72	18.10	154.78	138.16	9.57	0.05
4MMM	6.84	11.07	1.91	27.98	56.59	51.34	6.28	0.11
MMOO	6.81	11.65	0.15	41.34	137.86	118.48	0.55	0.00
MMHO	6.81	11.61	9.78	37.91	145.15	126.92	0.73	0.00

Table C-I. (Continued)

Glass	pH init	pH final	Leachate concentration (ppm) corrected for blanks (Values are averages of 3 measurements)					
			B	Si	Na	Na*	Al	Pb
2LOHZ	6.84	11.49	0.09	16.73	12.99	12.62	4.82	0.04
2HHOZ	6.84	11.52	21.87	124.82	223.41	185.02	0.17	0.30
4HOOA	6.81	11.40	0.30	44.27	112.71	99.00	0.20	0.00
4LOOE	6.81	10.35	0.09	39.59	27.98	27.97	0.26	0.00
4LHOE	6.60	9.75	4.58	34.52	19.67	17.71	0.25	0.30
4HHOE	6.77	11.10	15.13	79.87	142.16	121.36	0.55	0.00
5LOO	6.77	11.74	0.59	11.69	132.91	107.00	0.24	0.02
5HHO	6.77	12.33	12.99	147.61	1070.49	793.60	0.39	0.30

* Na by atomic absorption

Table C-II. Product Consistency Test Data. The tests were performed on glasses from the compositional space with results reported in log10 Normalized Release, NRi (mg/L)

Glass	B	Si	Na	Al	Pb	Fe	Ca	Ni	Ba
1,2MMH	1.821	1.850	2.663	1.897	0.801	0.000	1.892	0.000	1.795
1LOO		2.266	3.993		2.410	0.000	0.785	0.477	1.950
1HOO		3.236	4.298		3.439	1.749	0.560	0.521	2.132
1LHO	3.217	1.710	3.735		2.134	0.000	1.345	0.481	2.359
1HHO	4.318	3.659	4.604		3.130	1.493	0.000	0.488	1.688
1LOH		1.788	2.856	2.089	0.681	0.000	1.745	0.000	1.621
1HOH		2.479	4.629	3.801	3.320	1.538	1.513	1.546	1.190
1LHH	2.168	1.643	2.945	2.220	1.063	0.000	2.143	0.543	2.111
1HHH	3.817	2.657	4.404	3.682	3.174	1.836	1.262	1.858	1.539
2MMM	1.702	1.793	2.465	1.647	0.329	0.000	1.947	0.000	1.801
2LOO		2.018	2.601		0.000	0.000	2.138	0.000	2.264
2HOO		2.305	3.407		1.573	0.000	1.468	0.519	2.116
2LHO	2.101	2.140	2.613		0.949	0.000	2.282	0.521	2.388
2HHOZ	2.367	2.409	2.998		0.953	0.000	1.980	0.622	2.250
2HHO	2.518	2.534	3.181		0.953	0.000	1.691	0.515	2.003
2LOHZ		1.562	2.151	1.516	0.119	0.000	1.769	0.000	1.467
2LOH		1.550	2.117	1.506	0.000	0.000	1.743	0.000	1.441
2HOH		1.824	2.760	1.823	0.807	0.000	1.847	0.000	1.594
2LHH	1.562	1.556	2.116	1.554	0.975	0.000	1.853	0.548	1.452
2HHH	1.738	1.784	2.513	1.804	0.423	0.008	1.896	0.000	1.432
3MMM	2.117	1.960	2.949	2.207	0.232	0.000	1.758	0.000	1.648
3LOO		1.820	2.505		1.037	0.000	2.097	0.609	1.595
3HOO		2.637	3.881		1.823	0.837	0.647	0.647	1.055
3LHO	1.843	1.847	2.455		1.039	0.000	1.995	0.612	1.894
3HHO	2.579	2.494	3.489		1.044	0.495	1.054	0.616	0.783
3LOH		1.782	2.186	1.902	0.000	0.000	1.760	0.000	1.373
3HOH		2.860	4.165	3.161	2.555	0.798	1.678	1.635	1.534
3LHH	1.975	1.675	2.506	2.241	0.000	0.656	2.091	0.000	1.645
3HHH	3.469	2.495	4.155	3.329	2.676	0.787	1.526	0.637	1.706
4MMM	1.763	1.919	2.822	2.026	0.630	0.421	1.615	0.585	1.184
4LOOE		1.981	2.720		0.000	0.866	1.381	0.000	1.001
4LOO		1.910	2.513		0.000	0.793	1.489	0.000	1.109
4LHOE	1.830	1.993	2.525		1.043	0.850	1.738	0.622	1.467
4LHO	1.702	1.858	2.448		1.043	0.875	1.848	0.615	1.634
4HOO		2.072	2.907		1.041	0.036	1.289	0.613	0.777
4HHO	2.206	2.201	2.941		0.000	0.207	1.029	0.000	0.323
6LOH		1.622	2.473	1.647	0.000	0.624	1.672	0.000	1.290
6LHH	1.567	1.618	2.290	1.668	0.000	0.983	1.750	0.000	1.289
6HOH		1.798	2.585	1.846	0.000	0.148	1.592	0.000	0.980
6HHH	1.732	1.797	2.454	1.877	0.000	0.293	1.646	0.000	0.968

Table C-II.(Continued)

Glass	B	Si	Na*	Al	Pb	Fe	Ca	Ni	Ba
MID1	1.743	1.789	2.702	1.882	0.000	0.000	1.709	0.000	1.609
MID2	1.828	1.784	2.654	1.869	0.000	0.000	1.643	0.000	1.535
MID3	1.867	1.834	2.696	1.927	1.009	0.000	1.562	0.581	1.448
MMHO	2.165	2.039	2.915		0.000	0.000	1.254	0.000	1.268
MMOO		2.005	2.882		0.000	0.000	1.086	0.000	1.219
4HHOE	2.351	2.359	3.062		0.000	0.000	0.000	0.000	0.029
4HOOA		2.032	2.970		0.000	0.163	1.120	0.000	0.880

*Na by atomic absorption and all other elements by ICP.

Table C-III. Plot of PCT results for the 1-Space. Units in Log_{10} Normalized Release (mg/L)

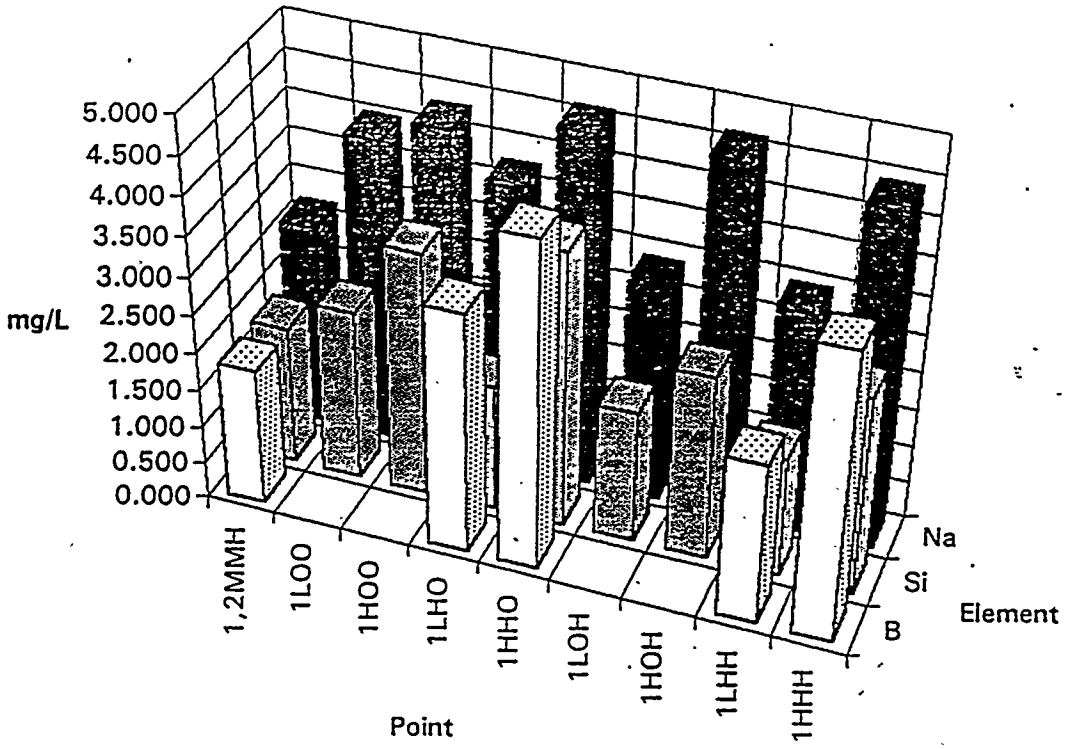

Table C-IV. Plot of PCT results for the 2-Space. Units in Log_{10} Normalized Release (mg/L)

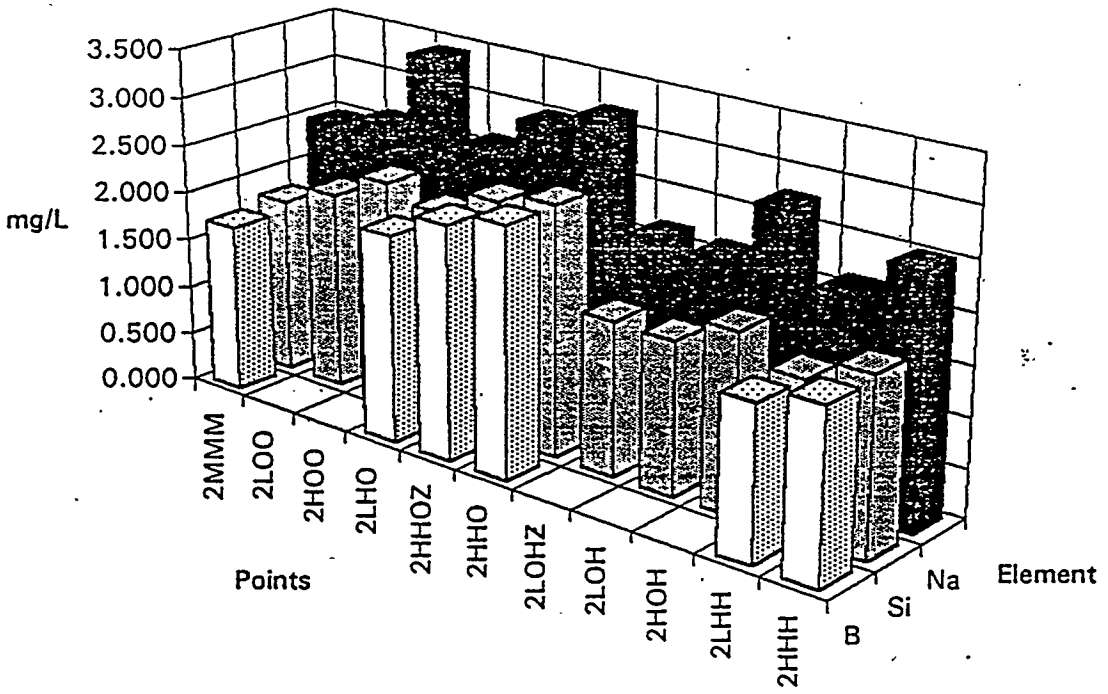

Table C-V. Plot of PCT results for the 3-Space. Units in Log_{10} Normalized Release (mg/L)

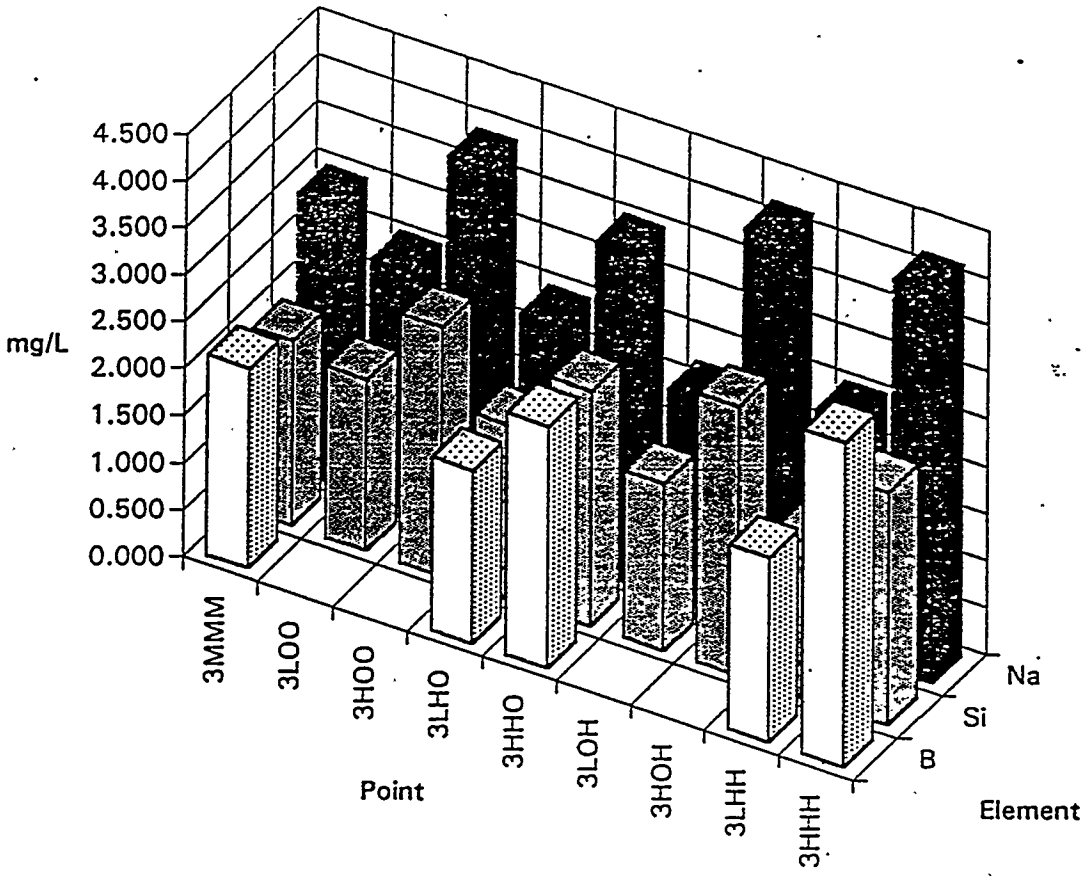

Table C-VI. Plot of PCT results for the 4-Space. Units in Log_{10} Normalized Release (mg/L)

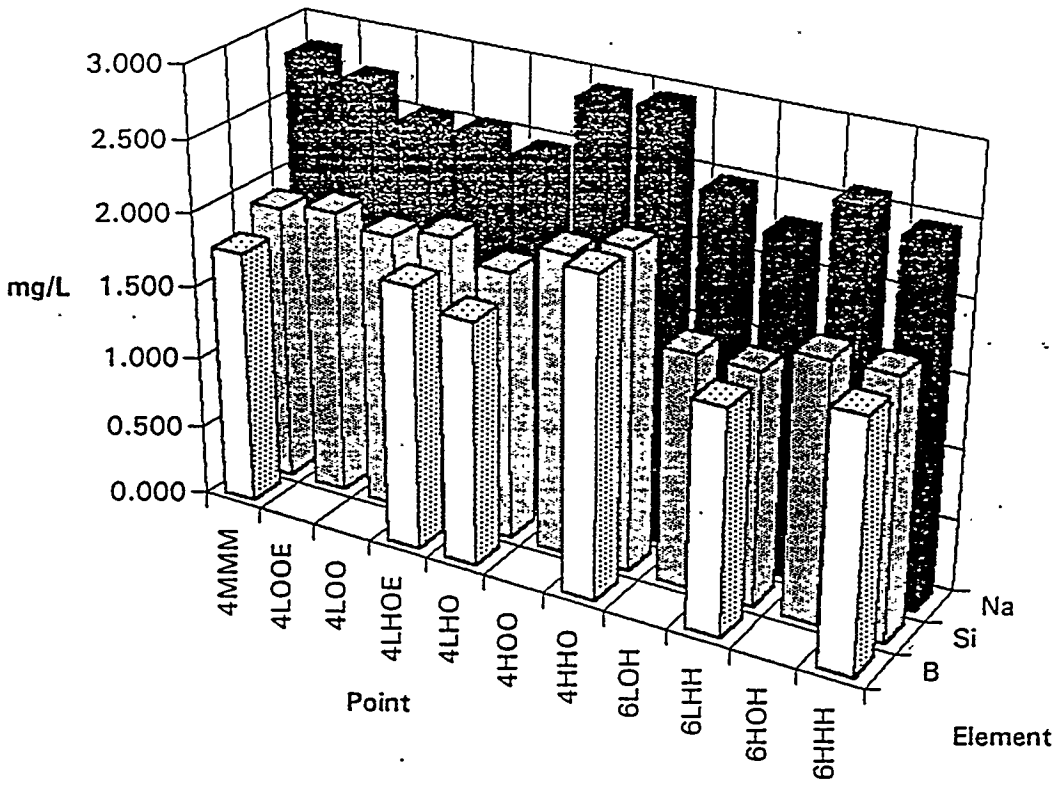

Appendix D

Iron Redox

The redox of the glasses has been determined by analyzing the Fe^{2+}/Fe^{3+} ratio. The redox analysis data for iron in the glasses appears in the following Table D-I. The WSRC Defense Waste Processing Facility (DWPF) uses redox ratios of 0.05 to 0.5 as one criteria to estimate if the manufactured glass will be durable (Jurgensen, 1994). The Fe^{2+}/Fe^{total} redox ratios for the 1-, 3-, and 4-spaces are all less than 0.3. The range of redox values for 2- space on the other hand ranged from 0.314 to 0.629. No explanation for this trend is given, but the effect is very pronounced

Table D-I. Redox Analysis Experimental Data

Glass	Fe^{2+}/Fe^{3+}	Fe^{2+}/Fe total	Glass	Fe^{2+}/Fe^{3+}	Fe^{2+}/Fe total
1LOO	0.304	0.233	3LOO	0.088	0.081
1LOH	0.362	0.266	3LOH	0.159	0.137
1LHO	0.268	0.211	3LHO	0.103	0.093
1LHH	0.424	0.298	3LHH	0.159	0.137
1HOO	0.195	0.163	3HOO	0.078	0.072
1HOH	0.264	0.209	3HOH	0.082	0.076
1HHO	0.189	0.159	3HHO	0.133	0.117
1HHH	NA	NA	3HHH	0.086	0.079
2LOO	0.639	0.390	4LOO	0.229	0.186
2LOH	1.320	0.569	4HOO	0.176	0.150
2LHO	1.050	0.512	4LHO	0.264	0.209
2LHH	0.620	0.383	4HHO	0.276	0.220
2HOO	0.973	0.493	6LOH	0.275	0.220
2HOH	0.698	0.411	6HOH	0.203	0.170
2HHO	1.695	0.629	6LHH	0.297	0.230
2HHH	0.458	0.314	6HHH	0.245	0.220
MMHO	0.230	0.187	MID1	0.161	0.139
MMOO	0.299	0.230	MID2	0.143	0.125
2MMM	0.784	0.440	MID3	0.281	0.219
3MMM	NA	NA	2LOHZ	0.594	0.370
4MMM	0.240	0.190	2HHOZ	0.846	0.458
1,2MMH	0.539	0.350			

NA = Not Analyzed

Appendix E

X-Ray Diffraction

Powder XRD was performed on 13 of the 43 glasses. Small low intensity lines were found for all the 3-Space glasses but for none of the other glasses. Optical microscopic examination of these glasses revealed the presence of dendritic crystals. It is believed that the minor crystalline phase may be trevorite, an iron-nickel spinels.

Appendix F

Glass Sampling from a Pilot-Scale Melter

About half way through the project, after the disk pouring and annealing process were proven, glass samples for XRF analysis were obtained directly from the Clemson University pilot-scale cold top melter during vitrification of an M-area surrogate sludge. This was accomplished by allowing the molten glass to be cast directly into a preheated graphite mold. After the annealing period was completed, the disk was transported to the Electron Microscopy Department in Jordan Hall on the main Clemson University campus where a Phillips 1450 XRF spectrometer is located. XRF intensity data were acquired from the sample. Total elapsed time, not including transportation, was approximately one hour. This procedure meets the requirements of the first and second experimental objectives.

Appendix G

Miscellaneous

A short discussion will be undertaken here to explain the rationale behind picking the type of mold to produce the XRF disks and to explain the success of the annealing process.

Several factors impacted the decision to use 40 mm high-purity graphite molds instead of platinum for preparation of the XRF samples. First, the precision study indicated that reasonable data precision could be expected using graphite molds. Second, using graphite crucibles would more closely approximate probable process conditions. Third, since polishing is such a simple and quick process, it could be accomplished at the melter site and would not significantly impact the total time required for an analysis if a decision was made to polish the samples. Fourth, in a process environment, the cost of graphite would be much less than the cost of platinum molds.

Of the approximately 220 disks cast, twelve cracked before the deliberate devitrification process (one of thirty-two cracked during devitrification). All twelve disks, came from three compositional points (1HOH, 1HHH, and 3HOH) and cracking was attributed to the unusual elemental mixture of those poinst as opposed to the annealing procedure. Overall, about 98.2 percent of the disks did not crack. This provides positive evidence that the annealing technique developed in this research project is suitable for XRF glass sample preparation.

REFERENCES

Alvarez, M., "Glass Disk Fusion Method for the X-Ray Fluorescence Analysis of Rocks and Silicates," *Advances in X-Ray Analysis*, vol. 19, pp. 203-206, 1990.

Baumann, E.W., Coleman, C.J., Karraker, D.G., Scott, W.H., *Colorimetric Determination of Fe(II)/Fe(III) Ratio In Glass*, USDOE Report DPMS-87-18, Savannah River Laboratory, Aiken, SC, 1990.

Bennert, D.M., Overcamp, T.J., Sargent, T.N, Jr., Resce, J.L., and Bickford, D.F., *Pilot-Scale Vitrification Laboratory for Treatability Studies on Hazardous and Mixed Wastes*, Environmental and Waste Management Issues in the Ceramic Industry, G.B. Mellinger (ed.), Ceramic Transactions, vol. 39, pp. 129-137, American Ceramics Society, Westerville, OH, 1993.

Berstein, F., "Application of X-Ray Fluorescence to Process Control," *Advances in X-Ray Analysis*, vol. 5, pp. 486-499, 1962.

Bertin, E. P. , *Principles and Practice of X-Ray Spectrometric Analysis*, 2nd ed., Plenum Press, New York, 1970.

Birks, L. S. , *X-Ray Spectrochemical Analysis*, Interscience Publishers, New York, 1969.

Bostick, W. D., Hoffman, D. P., Stevenson, R. J., Richmond, A. A., *Surrogate Formulations for Thermal Treatment of Low-Level Mixed Waste, Part IV: Wastewater Treatment Sludges*, USDOE Report DOE/MWIP-18, Martin Marietta Energy Systems, Oakridge, TN, 1994

Carney, K.P., "Development of Real-Time Monitors for the Elemental Characterization of Slag and Process Off-Gases for the Plasma Hearth Treatment Program," Proceedings of the International Topical Meeting on Nuclear and Hazardous Waste Management, Spectrum 94, American Nuclear Society, La Grange Park, IL, pp. 336-342, 1994.

Carr-Brion, K. , *X-Ray Analyzers in Process Control*, Elsevier Science Publishers, Ltd., London, 1989.

Cicero, C. A., Bickford, D. F., Bennert, D. and Overcamp, T, *Rocky Flats Plant Precipitate Sludge Surrogate Vitrification Demonstration (U)*, Report WSRC-RP-93-DRAFT, Westinghouse Savannah River Company, Aiken, SC, 1993a.

Cicero, C. A., Bickford, D. F., Jantzen, C. M., Bennert, D. and Overcamp, T., *Savannah River Site Simulated M-Area Sludge Vitrification Demonstration (U)*, Report WSRC-RP-93-659, Westinghouse Savannah River Company, Aiken, SC, 1993b.

Cicero, C. A., *LANL TA-50 Simulated Sludge Crucible Studies (U)*, WSRC Memo dated May 4, 1994, Westinghouse Savannah River Company, Aiken, SC, 1994c.

Claisse, F., *Norelco Reporter*, vol. 4, No. 1, 1957.

Criss, J. W., "Fundamental Parameters Calculations on a Laboratory Microcomputer," *Advances in X-Ray Analysis*, vol. 23, pp. 93-97, 1980.

Criss, J. W., and Birks, L. S., "Calculation Methods for Fluorescent X-Ray spectrometry," *Analytical Chemistry*, vol. 40, pp. 1080-1086, 1968.

Criss, J. W., Personal Communication, Criss Software Company, August, 1994.

de Galan, L., "Atomic Spectrometry: A User's View," *Philosophical Transactions: Physical Sciences and Engineering*, vol. 333, no. 1628, pp. 5-12, 1990.

de Jongh, W. K., *X-Ray Spectrometry*, vol. 2, p. 151, 1973.

de Jongh, W. K., *X-Ray Spectrometry*, vol. 8, p. 52, 1979.

Federal Register, "Land Disposal Restrictions for Third Schedule Wastes, Final Rule," 55 FR 22627, 1990.

Jantzen, C.M. and Bibler, N.E., Product Consistency Test (PCT) for DWPF Glass: Part I. Test Development and Protocol, U.S. DOE Report DPST-87-575, E.I. DuPont deNemours & Co., Savannah River Laboratory, Aiken, SC, 1987.

Jurgensen, A., Personal Communication, Westinghouse Savannah River Company, August, 1994a.

Jurgensen, A., Personal Communication, Westinghouse Savannah River Company, August, 1994b.

Lachance, G. R. and Claisse, F., "A Comprehensive Alpha Coefficient Algorithm," *Advances in X-Ray Analysis*, vol. 23, pp. 87-92, 1980.

Lachance, G. R. and Traill, R. J., "A Practical Solution to the Matrix Problem in X-Ray Analysis," *Canadian Spectroscopy*, vol. 11, pp. 43-48, 1966.

Lucas-Tooth, H. J., and Pyne, C., "The Accurate Determination of Major Constituents by X-Ray Fluorescent Analysis in the Presence of Large Interelement Effects," *Advances in X-Ray Analysis*, vol. 7, p. 523, 1961.

Luedemann, G., Mann, D., and Hagan, R., "Graphite Fusion of Geological Samples," *Advances in X-Ray Analysis*, vol. 34, pp. 213-216, 1991.

Phase Diagrams for Ceramists, The American Ceramic Society, 2nd ed., vol.1, p. 228, 1969.

Rasberry, S. D. and Heinrich, K. F. G., "Calibration for Interelement Effects in X-Ray Fluorescence," *Analytical Chemistry*, vol. 46, pp. 81-89, 1974.

Resce, J.L., Ragsdale, R.G., Overcamp, T.J., Hallman, T., and Davis, D. H., "Laboratory-Scale Vitrification of a Chloride-Containing Simulant of Incinerator Blowdown," Proceedings of the 1994 International Incinceration Conference, Thermal Treatment of Radioactive, Hazardous Chemical, Mixed, Munitions, and Pharmaceutical Wastes, University of California, Irvine, pp. 603-608, 1994.

Resce, J.L., Ragsdale, R.G., Overcamp, T.J., Jurgensen, A., Cicero, C., and Bickford, D. F., "XRF in Waste Glass Analysis and Vitrification Process Control, Part 1: Sample Preparation and Measurement Precision," Presented at the 96th Annual Meeting of the American Ceramics Society, April 24-28, 1994, Indianapolis, IN, 1994.

Ryan, W. and Radford, C. , *Whitewares Production, Testing and Quality Control*, Pergamon Press., New York, 1987.

DISCLAIMER